Plant Biotechnology Journal Open Access

Plant Biotechnology Journal (2022) **20**, pp. 691–710 doi: 10.1111/pbi.13747

Genomic and GWAS analyses demonstrate phylogenomic relationships of *Gossypium barbadense* in China and selection for fibre length, lint percentage and *Fusarium wilt* resistance

Nan Zhao[1,†], Weiran Wang[2,†], Corrinne E. Grover[3,†], Kaiyun Jiang[1], Zhuanxia Pan[4], Baosheng Guo[5], Jiahui Zhu[2], Ying Su[1], Meng Wang[2], Hushuai Nie[1], Li Xiao[2], Anhui Guo[1], Jing Yang[2], Cheng Cheng[1], Xinmin Ning[2], Bin Li[1], Haijiang Xu[2], Daniel Adjibolosoo[1], Alifu Aierxi[2], Pengbo Li[4], Junyi Geng[5], Jonathan F. Wendel[3,*], Jie Kong[2,*] and Jinping Hua[1,*]

[1]*Joint Laboratory for International Cooperation in Crop Molecular Breeding, Ministry of Education/College of Agronomy and Biotechnology, China Agricultural University, Beijing, China*

[2]*Institute of Economic Crops, Xinjiang Academy of Agricultural Sciences, Xinjiang, China*

[3]*Department of Ecology, Evolution and Organismal Biology, Iowa State University, Ames, IA, USA*

[4]*Institute of Cotton Research, Shanxi Agricultural University, Shanxi, China*

[5]*Cotton Research Institute, Hebei Academy of Agriculture and Forestry Sciences, Hebei, China*

Received 1 July 2021;
revised 22 October 2021;
accepted 27 October 2021.

**Correspondence* (Tel +86-10-62734748; fax +86-10-62734748; email jinping_hua@cau.edu.cn (J.H.); Tel +86-991-4504151; fax +86-991-4504151; email kongjie.258@163.com (J.K.); Tel +1-515-294-7172; fax +515-294-1337; email jfw@iastate.edu (J.F.W.))
[†]These authors are contributed equally.

Keywords: *Gossypium barbadense*, GWAS, fibre quality, yield, *Fusarium wilt* disease resistance.

Summary

Sea Island cotton (*Gossypium barbadense*) is the source of the world's finest fibre quality cotton, yet relatively little is understood about genetic variations among diverse germplasms, genes underlying important traits and the effects of pedigree selection. Here, we resequenced 336 *G. barbadense* accessions and identified 16 million SNPs. Phylogenetic and population structure analyses revealed two major gene pools and a third admixed subgroup derived from geographical dissemination and interbreeding. We conducted a genome-wide association study (GWAS) of 15 traits including fibre quality, yield, disease resistance, maturity and plant architecture. The highest number of associated loci was for fibre quality, followed by disease resistance and yield. Using gene expression analyses and VIGS transgenic experiments, we confirmed the roles of five candidate genes regulating four key traits, that is disease resistance, fibre length, fibre strength and lint percentage. Geographical and temporal considerations demonstrated selection for the superior fibre quality (fibre length and fibre strength), and high lint percentage in improving *G. barbadense* in China. Pedigree selection breeding increased *Fusarium wilt* disease resistance and separately improved fibre quality and yield. Our work provides a foundation for understanding genomic variation and selective breeding of Sea Island cotton.

Introduction

Cotton (*Gossypium* spp.) production accounts for a majority of natural textile fibres produced worldwide (Zhang *et al.*, 2014). While cotton has been domesticated independently four different times on two different continents, it is the two cultivated polyploid species (*i.e. G. hirsutum*, AD_1, and *G. barbadense*, AD_2) (Grover *et al.*, 2020; Wendel and Grover, 2015) from Central and Northern South America that predominate in modern cotton commerce. These species are derived from a single allopolyploidization event approximately 1.5 million years ago that subsequently radiated into the seven known polyploid species (Wang *et al.*, 2018). One of the polyploid species derived from this event, *that is G. barbadense*, is well known for its excellent fibre quality (Wang *et al.*, 2019), particularly its superior extra-long fibres (Yu *et al.*, 2013). Increasing demand for high-quality textiles has generated interest in understanding the genetics controlling fibre-related traits, particularly in Sea Island cotton, with the ultimate goal of genome-assisted breeding.

Both *G. hirsutum* and *G. barbadense* are allopolyploids derived from the union of two diploid genomes, A and D. The rapid development and application of genome sequencing technology to *Gossypium* have generated numerous insights into cotton genomics. The Peruvian diploid *G. raimondii* (D_5) was the first cotton genome to be sequenced (Paterson *et al.*, 2012; Wang *et al.*, 2012), followed by genome assemblies of some (Udall *et al.*, 2019) and resequencing of all 13 D-genome species (Grover *et al.*, 2019). Similarly, genome assemblies and resequencing data sets have been published for the A-genome diploids, *G. arboreum* (A_2) (Du *et al.*, 2018; Huang *et al.*, 2020; Li *et al.*, 2014) and *G. herbaceum* (A_1) (Huang *et al.*, 2020). Genomic resources are also available for the allopolyploids, including nine genome assemblies of *Gossypium hirsutum* (AD_1) genome (Chen *et al.*, 2020; Hu *et al.*, 2019; Huang *et al.*, 2020; Li *et al.*, 2015; Wang *et al.*, 2019; Yang *et al.*, 2019; Zhang *et al.*, 2015) and four of *G. barbadense* (AD_2) (Chen *et al.*, 2020; Hu *et al.*, 2019; Wang *et al.*, 2019; Yuan *et al.*, 2015), as well as thousands of resequenced accessions from both species

(Abdullaev *et al*., 2017; Cai *et al*., 2017; Dong *et al*., 2019; Fang *et al*., 2017a, 2017b, 2021; Huang *et al*., 2017; Islam *et al*., 2016; Li *et al*., 2018; Liu *et al*., 2018; Ma *et al*., 2018a, 2018b, 2019; Su *et al*., 2016, 2018; Sun *et al*., 2017; Tyagi *et al*., 2014; Wang *et al*., 2017a; Yuan *et al*., 2021; Zhao *et al*., 2014).

These many genomic resources have accelerated the identification of important genomic variations, including genes associated with important agronomic traits using genome-wide association studies (GWAS) in crop plants (Huang and Han, 2014; Huang *et al*., 2010, 2012; Jia *et al*., 2013; Li *et al*., 2013; Mace *et al*., 2013; Yano *et al*., 2016). While genome-wide studies in cotton have recently become more abundant (Abdullaev *et al*., 2017; Cai *et al*., 2017; Dong *et al*., 2019; Fang *et al*., 2017a, 2017b, 2021; Huang *et al*., 2017; Islam *et al*., 2016; Li *et al*., 2018; Liu *et al*., 2018; Ma *et al*., 2018a, 2018b; Su *et al*., 2016, 2018; Sun *et al*., 2017; Tyagi *et al*., 2014; Wang *et al*., 2017a; Yuan *et al*., 2021; Zhao *et al*., 2014), those focused on *G. barbadense* were few and involved limited sampling encompassing relatively little variation (Abdullaev *et al*., 2017; Fang *et al*., 2021; Su *et al*., 2020).

In addition, pedigree genomic analyses have been valuable in understanding selection for agronomic traits (e.g. fibre quality) in Upland cotton (*G. hirsutum*) (Lu *et al*., 2019; Ma *et al*., 2019). Lu *et al*. (2019) discovered hundreds of genes affecting tolerance to *Verticillium wilt*, salinity and drought and a block in a pedigree centred on CRI-12, whereas Ma *et al*. (2019) employed pedigree analysis to identify a key lint percentage-related gene (*GhWAKL3*) in the parents and progenies of Ekangmian 9. To date, there have been no pedigree-based inferences reported in Sea Island cotton.

Gossypium barbadense is originated from coastal Peru at least 7800 years ago, was initially domesticated in north-western South America, was diffused into Argentina-Paraguay and eastern and northern South America, and subsequently was expanded into Central America, the Caribbean and the Pacific (Percy and Wendel, 1990; Splitstoser *et al*., 2016; Westengen *et al*., 2005). Modern elite *G. barbadense* cultivars were developed on the coastal islands of Georgia and South Carolina, USA, and were later improved as Egyptian cotton and Pima cotton (Wendel *et al*., 2010). The earlier American Sea Island gene pool is the foundation of the Egyptian cottons, which were reintroduced into the USA as a part of the genetic base of the Pima cottons (Ulloa *et al*., 2009). The ancestors of the Egyptian, Egyptian-American and/or American germplasm were used in the development of the Turkmen and Uzbek *G. barbadense* germplasm (Abdullaev *et al*., 2017). In China, the main Sea Island cotton-growing area is in Xinjiang, where the initial parents were introduced from Central Asia, including Tajikistan, Uzbekistan and Turkmenistan. However, the understanding of phylogeny, geography, introduction and breeding of *G. barbadense* in China is mostly unexplored.

Studies on the important loci and genes responsible for fibre quality, yield and *Fusarium wilt* resistance of Sea Island cotton were few compared with those of upland cotton. Fan *et al*. (2018) first reported 24 QTLs for fibre quality and 18 QTLs for lint yield traits in 143 recombinant inbred lines (RILs) developed by Chinese *G. barbadense* cultivar 5917 and American *G. barbadense* cultivar Pima S-7 using GBS-SNPs. Yao *et al*. (2019) found that many *Fov*-induced lncRNAs were highly enriched in disease resistance-related pathways, including glutathione metabolism, glycolysis, plant hormone signal transduction, anthocyanin biosynthesis and butanoate metabolism, using transcriptome sequencing of four different Sea Island cotton RILs with susceptible, highly susceptible, highly resistant or super highly resistant phenotypes. Su *et al*. (2020) screened an E3 ubiquitin-protein ligase gene, *GB_A03G0335,* which was correlated with fibre length and strength, via GWAS analyses using 6309 SNPs from 279 Sea Island cotton accessions. Yu *et al*. (2021) identified three fibre strength candidate genes, *HD16* (*GB_D11G3437*, encoding casein kinase I isoform delta-like protein), *WDL2* (*GB_D11G3460*, encoding WDL1/WVD2-LIKE 1 protein, functioning in bundling microtubules) and *TUBA1* (*GB_D11G3471*, encoding tubulin alpha-1 chain protein), and one lint percentage candidate gene, *HERK 1* (*GB_A07G1034*, encoding receptor-like protein kinase regulated by brassinosteroids and required for cell elongation) by GWAS of 240 Sea Island cotton accessions. Lu *et al*. (2017) identified three fibre strength related genes, *XLOC_036333* (*MNS1*, encoding mannosyl-oligosaccharide-a-mannosidase), *XLOC_029945* (*FLA8*) and *XLOC_075372* (*snakin-1*), using transcriptome analyses on three chromosome segments substitution lines (CSSLs) derived from CCRI45 (*G. hirsutum*, recurrent parent) × Hai1 (*G. barbadense*). Four years later, Li *et al*. (2021) revealed another eight fibre-related genes that they separately encoded O-fucosyltransferase family protein (*GB_A02G0240*), glutamine synthetase 2 (*GB_A02G0272*), Ankyrin repeat family protein (*GB_A02G0264*), beta-6 tubulin (*GB_D03G1742*), WRKY DNA-binding protein 2 (*GB_D03G1655*), quinolinate synthase (*GB_D07G0623*), nuclear factor Y subunit B13 (*GB_D07G0631*) and leucine-rich repeat transmembrane protein kinase (*GB_D07G0797*), using the same materials and similar methods.

Here, we gained insights into the genotype-to-phenotype associations in *G. barbadense* using GWAS and a broad diversity of Sea Island cotton accessions, including a focus on lineages from China. We resequenced and phenotyped 336 Sea Island cotton accessions grown across 6 years and 4 locations to provide information on both genomic and phenotypic variations. Using these data, we performed GWAS for 15 important agronomic traits, including fibre quality, yield, resistance to *Fusarium wilt* disease, maturity-related traits and plant architecture, confirming the roles of five candidate genes responsible for four key traits using RNA-seq and transgenics. Finally, we explored the genetic basis for the improvement of Sea Island cotton through pedigree analysis, identifying elite genes involved in fibre length and lint percentage. Our results provide a foundation for Sea Island cotton improvement and molecular perspectives into cotton breeding.

Results

Genomic variation and population structure

We generated 9.4 Tb high-quality resequencing data involving 336 accessions derived from Asia (274), Africa (32), the Americas (28) and Europe (2) (Table S1 and Figure S1). Approximately 98.77% of reads covered 97.09% of the reference genome (Wang *et al*., 2019), with an average of 11.2-fold depth (Tables S1 and S2). We identified 16.0 million (M) single nucleotide polymorphisms (SNPs; Table 1 and Table S3) and 2.3 M insertion/deletion polymorphisms (InDels; Table S4). We found that the number of SNPs in At was approximately 1.8 times that found in Dt (Table S5 and Figure S2a), congruent with the twofold size difference between the At and Dt subgenomes (Li *et al*., 2014). SNP density was 1.8 SNPs/kb in At and 1.9 SNPs/kb

Table 1 Summary of classified SNPs

SNP category	No. of SNPs
Upstream	335 871
Exonic	
Stop gain	5057
Stop loss	514
Synonymous	86 767
Nonsynonymous	160 616
Intronic	524 253
Splicing	1666
Downstream	270 135
Upstream/downstream	25 959
Intergenic	14 429 742
Ts	10 789 456
Tv	5 242 423
Ts/Tv	2
Total	16 031 879

in Dt (Table S5 and Figure S2a), like that in *G. hirsutum* (Ma *et al.*, 2018). Diversity (θ_π) within the two subgenomes was similar, albeit slightly lower for Dt (5.3×10^{-4}) than At (6.2×10^{-4}) (Table S5 and Figure S2a), which agrees with a recent report (Yuan *et al.*, 2021).

For structure analysis, the natural logarithms of probability data (LnP(K)) and the *ad hoc* statistic ΔK were calculated (Dong *et al.*, 2019; Huang *et al.*, 2017; Su *et al.*, 2018). The Ln*P*(D) value increased continuously from $K = 1$ to 7 without an obvious inflection point (Figure S2b). However, the ΔK value showed a spike at $K = 2$ (Figure S2c). This suggested two major gene pools, consistent with the phylogenetic tree (Figure 1a), population structure analysis (Figure 1b and Table S6) and principal component analysis (PCA; Figure S2d). Given intraspecies introgression due to geographic distribution and breeding practice, some landraces and transitional accessions were integrated into a third mixed subgroup by increasing a new middle level of ancestry proportion at $K = 2$ (at first, when the ancestry proportion of one accession belonging to K1 was over 0.7, it was categorized as pop1, otherwise pop2, and then, accessions with the ancestry proportion from 0.5 to 0.7 were assigned into the mixed subpopulation; Figure 1c, Figure S2e–f and Table S7). Hereafter, these subgroups were designated as ‘Pop1’ (76), ‘mixed’ (91) and ‘Pop2’ (169 accessions; Table S6 and Figure S1). Pop1 primarily included recently selected cultivars from China’s northwest inland cotton region, with longer and stronger fibres (fibre length, FL mean = 42.47 mm; fibre strength, FS mean = 43.63 cN/tex). The ‘mixed’ population mainly included landraces from major cotton-planting areas in China, and transitional cultivars from other global cotton-producing countries, with medium-quality fibres (FL mean = 37.12 mm; FS mean = 37.97 cN/tex). Pop2 contained most of the earlier varieties from cotton-producing countries worldwide, with shorter and lower-strength fibres (FL mean = 36.29 mm; FS mean = 36.54 cN/tex).

Among all accessions, θ_π value was 5.84×10^{-4} on average, ranging from 4.96 to 5.74×10^{-4} across the three subpopulations (Figure 1d). This is similar to the overall diversity in a set of Chinese-focused Upland cotton accessions (5.39×10^{-4}; Wang *et al.*, 2019). Genetic differentiation (F_{ST}) values among the three subpopulations were 0.049–0.155 (Figure 1d), like that previously found in Upland cotton (Fang *et al.*, 2017b; Ma *et al.*, 2018b). The decay rate of linkage disequilibrium (LD), that is the pairwise correlation coefficient (r^2) from the maximum value to the half-maximum, was 388 kb for all 336 accessions and was close among populations (i.e. 373, 342 and 342 kb for Pop1, mixed and Pop2 respectively; Figure 1e). These LD values were higher than that of Upland cotton reported by Wang (296 kb; Wang *et al.*, 2017a), but lower than that of Fang (1000 kb; Fang *et al.*, 2017b).

Genome-wide association studies identification

We measured 15 traits (Table 2), including fibre quality (five), yield components (five), disease resistance (one), maturity (two) and plant architecture (two; Table 2), for the 336 Sea Island cotton accessions grown across four locations over six years (Table S8). Diverse phenotypic variations were observed for all traits (Table 2 and Table S9). Two of the fibre quality traits important for the spinning industry, FL and FS, were positively correlated with six traits FU, BN, FBN, SBW, SI and PH, while also being negatively associated with the other seven traits (i.e. FM, FE, LP, DP, GP, FNFB and FBT; Figure S3). Using 4.1 M high-quality SNPs, we performed GWAS for these 15 traits. These analyses revealed 6,241 unique SNPs, including 437 same SNPs among different traits (Figure S4–S18, Table S10 and S11). The number of significant SNP varied among traits, for those were selected and improved by emphasis in our population, and the numbers of significantly associated SNPs were relatively large. For example, DP had the greatest number of associated SNPs, followed by two fibre quality traits (i.e. FM and FS). For traits that the selection and improvement degree were relatively low, their numbers of significant SNPs were small, such as LP, FU, FL, SI, FBT, SBW and so on. Generally, the effective candidate regions with significant GWAS signals were defined as the LD blocks surrounding the signal peak (Yano *et al.*, 2016), although these were sometimes enlarged slightly when candidate genes could not be identified (Fang *et al.*, 2017b). Based on the 388 kb LD decay distance and candidate gene analysis, we defined 500 kb (slightly larger than 388 kb) upstream and downstream of a significant SNP signal peak (i.e. totally 1-Mb interval; Fang *et al.*, 2017b) as the candidate region size and found 18 696 unique genes, involving in 6183 common genes related to at least two traits (Table S10 and S12). The total number of associated genes was highest for the fibre quality category, followed by maturity. From these, we chose key genes related to four agronomically important traits for further functional verification.

Fibre length

On chromosome A05, we identified one nonsynonymous SNP, within the candidate region located at 16.28–16.30 Mb, significantly correlated with fibre length (Figure 2a,b). The gene containing this SNP, *Gbar_A05G017500*, encoded a predicted U-box domain-containing E3 ubiquitin ligase (PUB4), named after *FIBER LENGTH2* (*GbFL2*). The phenotypically associated SNP (16286973) resulted in a T/G transversion, leading to leucine (L) or valine (V) (Figure 2c), which was associated with either longer (T) or shorter (G) fibre respectively (Figure 2d). While most of the early introduced varieties in Pop2 had the long-fibre haplotype (T; Figure 2e), the proportion of short-fibre haplotypes (G) raise up to near equivalence in the ‘mixed’ population (Figure 2e), perhaps due to linkage drag associated with selection on other traits. The long-fibre (T) haplotype gained prominence again in Pop1, comprising 83.33% of haplotypes for this locus (Figure 2e).

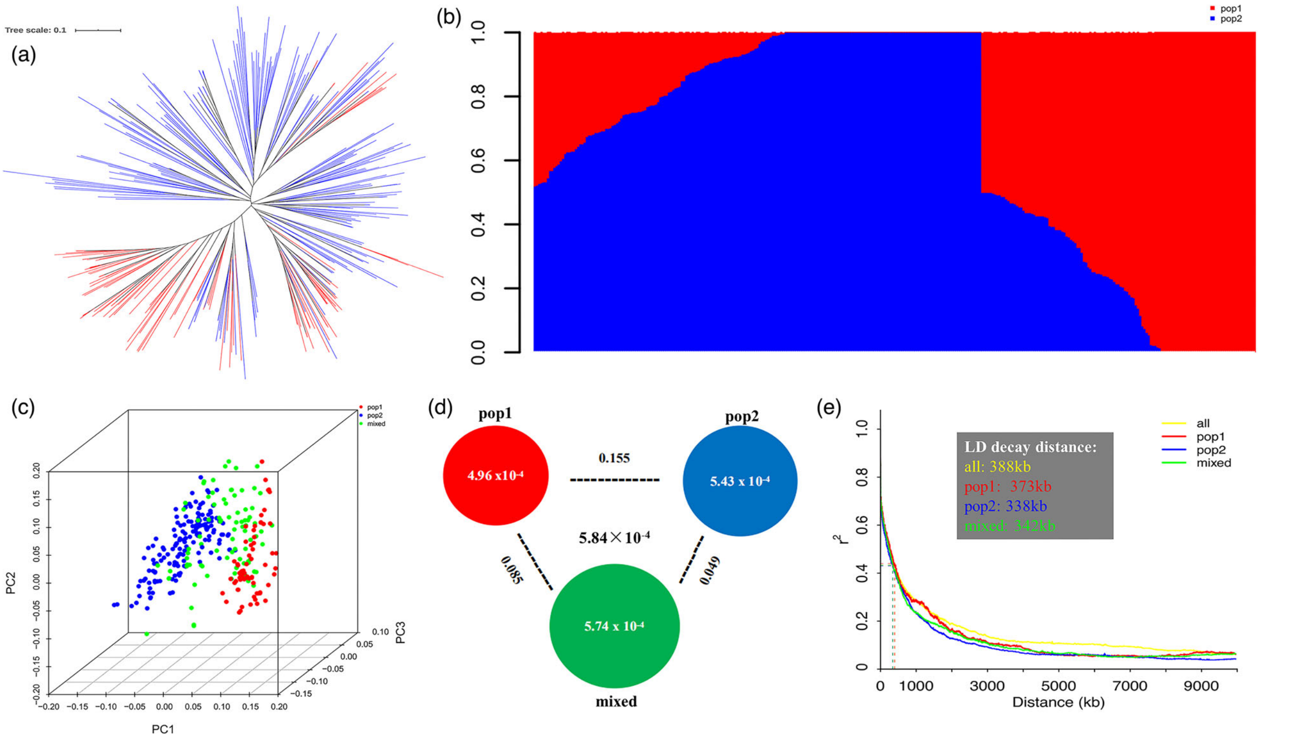

Figure 1 Phylogeny, structure, PCA, diversity and LD decay of 336 Sea Island cotton accessions. (a) Phylogenetic neighbour-joining tree based on 3.5 M high-quality genomic SNPs. The accessions in primary pop1 and pop2 are in red and blue respectively. (b) Structure analysis with $K = 2$. The *y*-axis quantifies cluster membership, and the x-axis represents different accessions. (c) PCA plot of the first three components for three subpopulations. (d) Genetic diversity and population differentiation across the three groups. The values in the circles are genetic diversity ($\theta\pi$) of the groups (red, blue and green circles represent pop1, pop2 and mixed groups respectively), and the values between the groups quantify population differentiation (F_{ST}). (e) Genome-wide average LD decay in pop1, pop2 and mixed.

Expression of *GbFL2* gradually decreased during fibre development (from 0 DPA to 20 DPA) and was lower in long-fibre varieties (Figure 2f). We validated expression pattern of *GbFL2* using qRT-PCR in FL extreme accessions (Figure 2g), namely, a negative regulation pattern. VIGS transformation of *GbFL2* in high and low FL lines showed increased fibre length relative to the wild type (Figure 2h-i), supporting the role of *GbFL2* in fibre elongation. *GbFL2* is derived from the At chromosomes (i.e. A05) of AD_2 (Figure 2j), and the change in haplotype frequency during breeding is suggestive of directional selection during domestication (Figure 2k and Table S14).

Fibre strength

On chromosome D11, we identified one nonsynonymous SNP significantly correlated with fibre strength in the candidate locus at 64.20–64.25 Mb (Figure S19a-b). The sole gene contained within this locus, *Gbar_D11G032670*, encoded a putative casein kinase 1-like protein (HD16), named after *FIBER STRENGTH1* (*GbFS1*). The two alleles (C/T) detected at this position (D11:64227153) encoded two different amino acids, threonine (T) and isoleucine (I; Figure S19c), corresponding to low (C haplotype) and high fibre strength (T haplotype; Figure S19d). The early introduced varieties from Pop2 had the high-strength fibre haplotype (T), and the change in allele frequency hinted at directional selection during breeding in China (vs mixed and Pop1; Figure S19e). Of the 159 Chinese accessions, 144 contained the T/G haplotypes for *GbFL2* and T/C for *GbFS1* (the remaining 15 were missing information/nucleotides or had unique mutations; Figure S20 and Table S13). Among those 144 accessions, 41 accessions had the long/high-strength haplotype combination (TT), 35 exhibited short/low strength (GC), 58 had long/low strength (TC) and 10 exhibited short/high strength (GT). This suggested that although fibre length and strength were often regarded as the simultaneous targets of selection, Sea Island cotton breeding in China might have favoured fibre length as a priority (99 versus 45 accessions; Figure S19e). *GbFS1* was highly expressed at most fibre developmental stages (5-20 DPA; Figure S19f) in low strength accessions, implying a negative regulation pattern (Figure S19f-g). *GbFS1* was derived from the Dt subgenome (i.e. chromosome D11) of AD_2, having been inherited from the D-genome ancestor (represented by the D_5 genome, Figure S19h), which is notable in that D-genome species have short, non-spinnable fibres. Interestingly, Dt homeolog of *GbFS1* showed directional selection in AD_2 relative to their AD_1 counterpart, suggesting selection of this advantageous mutation in Sea Island cotton (Figure S19h–i and Table S14).

Lint percentage

On chromosome A05, we also identified a strong signal associated with lint percentage (Figure 3a). The gene closest to this region (13.00–13.20 Mb), *Gbar_A05G014160*, had one nonsynonymous SNP (A05:13046765), that is a C/G transversion, resulting in an amino acid difference, that is either alanine (A) or glycine (G), the latter of which was associated with a significant improvement in lint percentage (Figure 3b–d). We designated the locus containing this gene *LINT PERCENTAGE*

Table 2 Summary of phenotypic data

Categories	Traits	Min	Max	Mean	SD	CV(%)	Skewness	Kurtosis
1. Fibre quality	1.1 Fibre length (FL, mm)	24.90	39.60	33.70	2.50	7.50	−0.23	0.16
	1.2 Fibre uniformity (FU, %)	80.00	90.00	85.70	1.80	2.10	−0.26	0.22
	1.3 Fibre strength (FS, cN/tex)	26.70	52.60	39.30	4.90	12.40	0.55	0.06
	1.4 Fibre elongation (FE, %)	5.30	10.00	7.00	0.70	9.90	0.52	2.56
	1.5 Fibre micronaire (FM)	2.90	5.30	4.00	0.40	10.70	0.21	0.18
2. Yield and yield composition factors	2.1 Fruit branch number (FBN)	5.50	15.40	10.50	1.70	16.60	0.01	−0.01
	2.2 Boll number (BN)	2.30	15.60	8.90	2.20	24.90	0.12	0.35
	2.3 Single boll weight (SBW, g)	2.00	4.00	3.10	0.30	11.10	0.02	0.28
	2.4 Lint percentage (LP, %)	25.00	41.00	32.80	2.60	8.10	0.24	0.30
	2.5 Seed index (SI, g)	9.10	14.80	11.70	1.00	8.70	0.13	−0.09
3. Disease resistance	3.1 Disease percentage (DP, %)	0.00	92.60	33.70	24.30	72.60	0.43	−0.70
4. Early maturity	4.1 Growth period (GP, day)	114.90	143.50	129.60	6.40	4.90	0.08	−0.83
	4.2 First node of fruit branch (FNFB, node)	2.00	6.70	4.10	1.10	25.80	0.41	−0.75
5. Plant architecture	5.1 Plant height (PH, cm)	35.80	133.50	73.20	15.80	21.80	0.57	1.21
	5.2 Fruit branch type (FBT)	0.00	3.20	1.00	1.20	123.20	0.52	−1.53

(*GbLP1*), which encoded a putative ATP-dependent RNA helicase (DEAH12) targeted to the chloroplast. This putative protein contained a RING-type zinc-finger domain, a characteristic of the E3 ubiquitin ligase RBR family. Unlike *GbFL2* and *GbFS1*, the number of accessions with high-lint-percentage haplotype (G) had generally been decreasing gradually since the first introduction of Sea Island cotton into China; however, the ratio of G/C fluctuated, first increasing and then decreasing (Figure 3e) in later accessions, as the need for greater lint production was balanced with fibre quality. High expression of *GbLP1* occurred at the whole fibre developmental stages, especially at 0 and 5 DPA (Figure 3f), consistent with qRT-PCR validation in LP extreme accessions (Figure 3g). VIGS transformation in LP extreme Sea Island cotton lines with matching G/C haplotypes showed decreased lint percentage (Figure 3h), confirming the role of *GbLP1* in lint-percentage forming. Like *GbFL2*, *GbLP1* showed signatures consistent with positive selection (i.e. A_2, Figure 3i–j and Table S14), while its homeolog (here, in the D_t genome) exhibits patterns consistent with purifying selection (Figure 3i,j and Table S14). Notably, most accessions had alleles conferring long fibre but with low strength and low lint percentage, followed by accessions exhibiting high lint percentage but with short fibre and low strength, implying the strongest directional selection was on long fibre, followed by high lint-percentage (Figure S20b and Table S13).

Fusarium wilt resistance

Cotton fusarium wilt disease, caused by the fungus *Fusarium oxysporum* f. sp. *vasinfectum* (FOV), is one of the most significant diseases impacting yield in *G. barbadense*. Here, we revealed a strong association signal cluster on chromosome D03 related to FOV disease percentage (DP) (Figures S21a; Figure 4a). We screened two closely linked candidate genes from this cluster, that is *Gbar_D03G001430* (henceforth *GbDP1*) and *Gbar_D03G001910* (*GbDP2*), at 0.8–1.0 Mb and 1.5–1.6 Mb respectively (Figure S21b; Figure 4b). *GbDP1* encoded a putative zinc-finger homeodomain rotein 6 (ZHD6), and *GbDP2* encoded a putative wall-associated receptor kinase-like 14 (WAKL14). Both *GbDP1* and *GbDP2* had a nonsynonymous A/C transversion in their coding sequences, which resulted in a lysine (K)–asparagine (N) (Figure S21c) and a serine (S)–arginine (R) shift (Figure 4c), respectively, whose close linkage generally resulted in two haplotypes (AA and CC). Accessions carrying the CC-haplotype showed significantly lower disease percentage than those with the AA-haplotype (Figures S21d; Figure 4dc). Most early introduced varieties had the high-disease-percentage haplotype (AA) (Figure S21e; Figure 4e); however, there had been 20 recently selected cultivars with low-disease-percentage haplotype (CC) in Xinjiang (in pop1) (Figures S20e; Figure 4e). Among the 178 Chinese Sea Island containing *GbDP1* and/or *GbDP2*, 164 (92%) contained AA (144) or CC (20) (Figure S20c and Table S13). Both *GbDP1* and *GbDP2* exhibited high expression in susceptible (S) lines after FOV inoculation (Figures S21f; Figure 4f), implying a negative regulation pattern. *GbDP1*/*2*-silencing in susceptible lines (S_pCLCrVA-*DP1*/S_pCLCrVA-*DP2*) conferred increased resistance to FOV infection relative to empty-vector-carrying (S_pCLCrVA) and wild-type cotton susceptible lines (S_WT) (Figure S21-h and Figure 4g,h). These results suggested that *GbDP1 and GbDP2* were two potential targets for conferring FOV resistance in *G. barbadense*. *GbDP1* orthologs in AD_2, AD_1 and D_8 were nearly identical but differed from the D_5 ortholog by two SNPs in a 423-bp conserved region (Figure S21i-j and Table S14). This might reflect introgression from D_8 into the AD_1-AD_2 lineage or, more likely, autapomorphic changes in the D_5 lineage after divergence from the (now extinct) D-genome donor parents of the allotetraploids. For *GbDP2,* the case was more complex, and there were four kinds of variations in a 1509-bp conserved region among the AD_2, AD_1, D_5 and D_8 homologues: (i) the homologue in AD_2 had three specific SNPs compared to those in AD_1, D_5 and D_8; (ii) the homologues in AD_2 and AD_1 had three common SNPs compared to those in D_5 and D_8; (iii) the homologues in AD_2, AD_1 and D_5 had five common SNPs compared to those in D_8; (iv) the homologues in AD_2, AD_1 and D_8 had two common SNPs compared to those in D_5. These data demonstrated differential SNP introgression from AD_1, D_5 and D_8 into AD_2, reflecting differential selection of *GbDP2* homologues after allotetraploidy (Figure 4i,j and Table S14). Despite the high level of conservation between AD_1-AD_2 for these two genes, evolution selection analyses of the Sea Island and Upland cotton D-homeologs suggested different histories of selection (Figure 4i,j, Figure S21i, j and Table S14). A simultaneous consideration of all four traits,

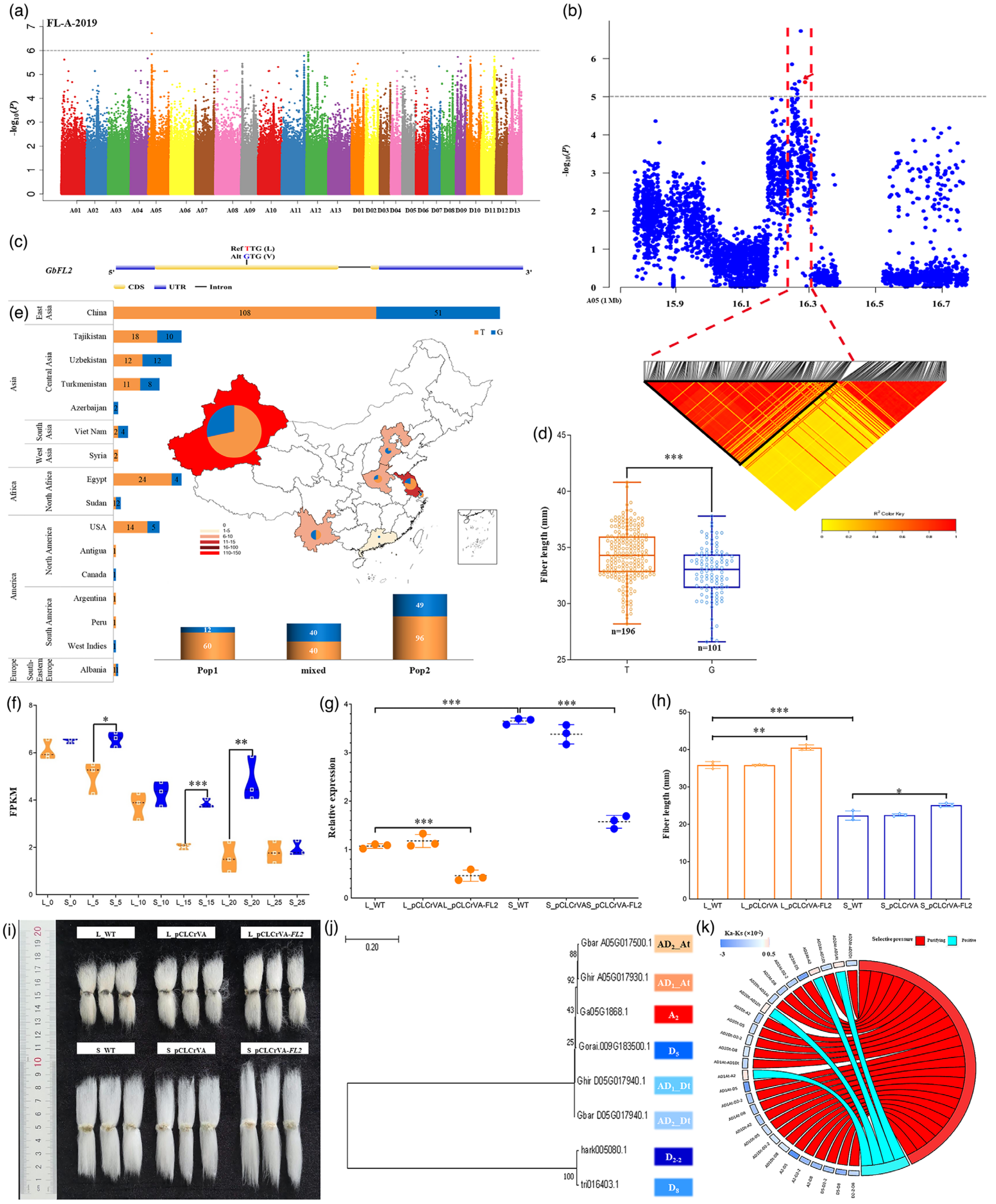

that is FL, FS, LP and DP, suggested priority selection on long fibre and high lint percentage once again (Figure S20d and Table S13).

Genomic characterization of a pedigree

We selected an intact pedigree from our GWAS population to examine the origin of two elite cultivars, XH39 and XH60, which were derived from the same initial breeding pool (11 common parents), but were later subjected to selection for longer fibre (in XH39) and high lint percentage (in XH60) respectively (Figures 5a–f and 6a–f). Comparisons among the parents and the two elite lines traced 4.57% and 3.78% of the genome in XH39 and XH60 respectively; through the historical crosses leading through these lineages, most of the traceable transmissions were

Figure 2 Identification of the FL causal gene *GbFL2* on chromosome At05. (a) Manhattan plot for FL. The dashed line represents the significance threshold (-$\log_{10}P = 6$). Effect values of genetic markers were tested using *F* tests and corrected for multiple testing using Bonferroni correction. (b) Local Manhattan plot (top) and LD heatmap (bottom) surrounding the peak on At05. The dashed line represents the significance threshold (-$\log_{10}P = 5$). Red arrows mark the position of the nonsynonymous SNP A05_16286973 in *Gbar_A05G017500* (*GbFL2*). Red dotted lines show the candidate region. (c) Structure of *GbFL2*. Blue and yellow rectangles mark UTR and CDS respectively. (d) Box plot for FL, based on the haplotypes of the two SNPs. In the box plots, the centre line indicates the median. Box limits are the upper and lower quartiles, and whiskers mark the range of the data; *n* denotes the number of accessions with the same genotype. We used a two-tailed *t*-test to perform the significance analysis. (e) Haplotype distribution in diverse geographical regions and subpopulations. The bar chart on the left shows the number of two haplotypes in distinct countries. The map in the middle displays the ratio of two haplotypes in the different provinces of China. The column diagrams below represent the number of two haplotypes in different subpopulations. (f) Expression of *GbFL2* in long-fibre accession XH58 (haplotype T) and short-fibre accession Ashi (haplotype G) at the fibre developmental stages (0, 5, 10, 15, 20, 25 DPA), detected by RNA-seq (FPKM value). Data are average values with standard deviation ($n = 3$ varieties with three technical repeats). Single (*), double (**) and triple (***) asterisks mark statistical significance levels of $P < 0.05$, 0.01 and 0.001 respectively. (g) qRT-PCR analysis of *GbFL2* expression in wild-type (WT), transgenic lines with empty VIGS vector (pCLCrVA) and target gene *GbFL2* (pCLCrVA-*FL2*) of long-fibre (L) accession XH58 and short-fibre (S) accession Ashi. The gene expression level in the long-fibre accession wild type (L_WT) was set to 1. *GbUBQ7* is an internal control. (h) Fibre length (mm) of WT, pCLCrVA, (pCLCrVA-*FL2* of long-fibre (L) accession XH58 and short-fibre (S) accession Ashi. (i) VIGS phenotypes of *GbFL2*. (j) The evolutionary origin of *GbFL2* (*Gbar_A05G017500*). We built unrooted trees using the maximum-likelihood method in MEGA7, based on complete CDS sequences. (k) Selection analysis on homologous CDS sequences of *GbFL2*. Homologous sequence in each cotton species is represented by its genome name on the left side of the circle. The difference value (Ka-Ks) of each group of homologous comparisons is indicated by coloured rectangles according to the colour bar in the upper left corner. While Ka/Ks is generally used as an indicator of selective pressure, the presence of 'Ks = 0' here precludes this; therefore, we chose another indicator, that is 'Ka-Ks' value. Two types of selection effects, purifying selection (in red) and positive selection (in blue), are shown on the right side of the circle.

found in the At genome (Figures 5a–d, 6a–d and Table S15). We then analysed the overlapping genes between our broader GWAS analysis and those regions whose genetic transmission was traceable across the pedigree. For XH39, we uncovered 32 and 178 genes controlling fibre length and strength in these overlapping regions (Figure 5g and Table S16), four of which simultaneously impacted FL and FS (Figure S22a and Table S16). Two of these four genes, *Gbar_A04G013270* and *Gbar_A04G013290*, had high expression at 5-25 DPA fibres with a positive-regulation pattern, especially at 10 and 15DPA fibres of long-fibre line (Figure 5h). These were specifically passed from parent 86430, notably, the accession with the longest fibre among the 13 parental lines (Figure 5i). *Gbar_A04G013270* encoded a triosephosphate isomerase, the key enzyme in glycolysis that produces energy, while *Gbar_A04G013290* was a newly annotated gene with no existing functional information (Table S16). For XH60, 70 LP-related genes overlapped between the GWAS and genetic transmission analyses (Figure 6g and Table S16). One of them, *Gbar_D04G017350,* had high expression during fibre development, with negative regulation in the earlier stage (0, 5, 10 and 15 DPA) (Figure 6h). Consistent with a negative regulation pattern, the parental origin of this gene, that is accession JH1, had the lowest lint percentage among the parents (Figure 6i). This gene (*Gbar_D04G017350*) encoded a tubulin alpha-2 chain, the major constituent of microtubules (Table S16). Additionally, there were 11 shared genes for the lint percentage and seed index traits (Figure S22b and Table S16). Attributable to their shared parental history, XH39 and XH60 both contained six, nine and one gene(s) simultaneously improving BW, GP and DP respectively (Figures 5f and 6f, Figure S22c and Table S16). Additional experiments are required to increase understanding of the roles of these genes.

Discussion

Genomic variations encoding phenotypic diversity

Association mapping was initially applied to Upland cotton in 2009 (Abdurakhmonov *et al*., 2009), first using SSRs (Abdurakhmonov *et al*., 2009; Tyagi *et al*., 2014; Zhao *et al*., 2014) and then GBS (Islam *et al*., 2016), SLAF-sequencing (Su *et al*., 2016, 2018), SNP arrays (Cai *et al*., 2017; Dong *et al*., 2019; Huang *et al*., 2017; Li *et al*., 2018; Liu *et al*., 2018; Ma *et al*., 2018b; Ma *et al*., 2018b) and whole-genome resequencing (Fang *et al*., 2017b; Sun *et al*., 2017; Wang *et al*., 2017a). In contrast, association studies in Sea Island cotton were few, consisting of only four publications (Abdullaev *et al*., 2017; Fang *et al*., 2021; Su *et al*., 2020; Yu *et al*., 2021). Here, we resequenced a large population consisting of 336 Sea Island cotton accessions and identified 9.4 Tb high-quality sequencing data. Like Upland cotton (Wang *et al*., 2017a), divergence among geographic groups of *G. barbadense* in China was more obscure than in other crop species (Huang *et al*., 2012; Zhou *et al*., 2015), although most accessions fall into one of two main populations whose genetic diversity varied by breeding history.

Phenotypic data for these diverse accessions were over nine original sets (locations × year) that surveyed 15 agronomically important traits and yielded several repeatedly detectable candidate genes suitable for follow-up analyses. Notably, although some studies on Sea Island cotton have been published (Abdullaev *et al*., 2017; Fang *et al*., 2021; Su *et al*., 2020; Yu *et al*., 2021), more than 80% of the accessions studied here are newly sequenced (Table S1, S17 and S18). Phenotypic differences among lines used in our and other reports were small, suggesting the congruence with previous surveys (Table S18; Fang *et al*., 2021; Su *et al*., 2020; Yu *et al*., 2021). Overlapping signals were detected between our and previous reports (Fang *et al*., 2021; Su *et al*., 2020; Yu *et al*., 2021), including 80 fibre-length and 112 strength genes in the overlapping regions (Table S19). Notably, the fibre length candidate gene characterized here, *Gbar_A05G017500* (*GbFL2*), had a homeolog in a previously identified fibre-length QTL region (TM10723_TM10747_TM10754; Su *et al*., 2020), and the fibre strength candidate, *Gbar_D11G032670* (*GbFS1*), was contained within a large SNP-cluster on chromosome D11 that was proximal to a previously identified fibre strength locus (loci24; Fang *et al*., 2021; Table S19). Additional evidence was that a *HD16* ortholog (*GB_D11G3437*) on chromosome D11 was found to be associated with fibre strength in 240 *Gossypium barbadense* accessions (Yu *et al*., 2021); this gene has 100% identity with our *GbFS1*, with the

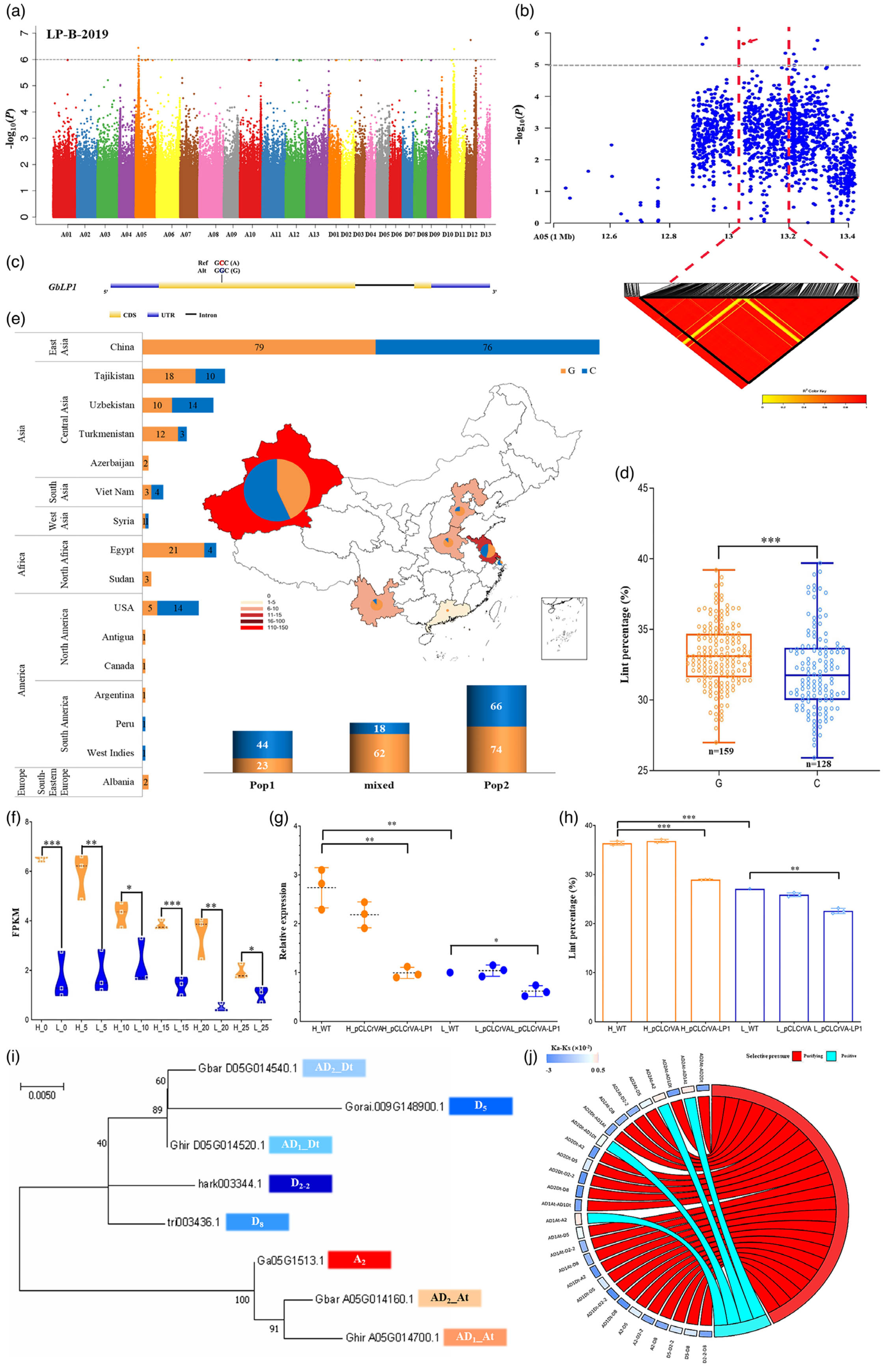
(a)
LP-B-2019
$-\log_{10}(P)$
A01 A02 A03 A04 A05 A06 A07 A08 A09 A10 A11 A12 A13 D01 D02 D03 D04 D05 D06 D07 D08 D09 D10 D11 D12 D13
(b)
$-\log_{10}(P)$
A05 (1 Mb)
12.6
12.8
13
13.2
13.4
R² Color Key
(c)
Ref GCC (A)
Alt GGC (G)
GbLP1
5'
3'
CDS
UTR
Intron
(e)
Asia
East Asia
China 79 76
Central Asia
Tajikistan 18 10
Uzbekistan 10 14
Turkmenistan 12 3
Azerbaijan 2
South Asia
Viet Nam 3 4
West Asia
Syria 1
Africa
North Africa
Egypt 21 4
Sudan 3
America
North America
USA 5 14
Antigua 1
Canada 1
South America
Argentina 1
Peru 1
West Indies 1
Europe
South-Eastern Europe
Albania 2
G
C
0
1-5
6-10
11-15
16-100
110-150
Pop1 44 23
mixed 18 62
Pop2 66 74
(d)
***
Lint percentage (%)
n=159
n=128
G
C
(f)
FPKM
***
**
*
***
**
*
H_0 L_0 H_5 L_5 H_10 L_10 H_15 L_15 H_20 L_20 H_25 L_25
(g)
Relative expression
**
**
*
H_WT H_pCLCrVAH_pCLCrVA-LP1 L_WT L_pCLCrVAL_pCLCrVA-LP1
(h)
Lint percentage (%)
***
***
**
H_WT H_pCLCrVA H_pCLCrVA-LP1 L_WT L_pCLCrVA L_pCLCrVA-LP1
(i)
0.0050
60
89
40
100
91
Gbar D05G014540.1 AD_2_Dt
Gorai.009G148900.1 D_5
Ghir D05G014520.1 AD_1_Dt
hark003344.1 D_{2-2}
tri003436.1 D_8
Ga05G1513.1 A_2
Gbar A05G014160.1 AD_2_At
Ghir A05G014700.1 AD_1_At
(j)
Ka-Ks (×10⁻³)
-3
0 0.5
Selective pressure
Purifying
Positive

Figure 3 Identification of the LP causal gene *GbLP1* on chromosome At05. (a) Manhattan plot for LP. The dashed line represents the significance threshold (-$\log_{10}P = 6$). Effect values of genetic markers were tested using *F* tests and corrected for multiple testing using Bonferroni correction. (b) Local Manhattan plot (top) and LD heatmap (bottom) surrounding the peak on At05. We use an *F* test to perform statistical analysis. The dashed line represents the significance threshold (-$\log_{10}P = 5$). Red arrows mark the positions of the nonsynonymous SNP A05_13046765, which is located within *Gbar_A05G014160* (*GbLP1*). Red dotted lines mark the candidate region. (c) Structure of gene *GbLP1*. Blue and yellow rectangles mark UTR and CDS respectively. (d) Box plot for LP, based on the haplotypes of the two SNPs. In the box plots, the centre line indicates the median. Box limits are the upper and lower quartiles, and whiskers mark the range of the data. *n* denotes the number of accessions with the same genotype. We use a two-tailed *t*-test to perform the significance analysis. (e) Haplotypes distribution in diverse geographical regions and subpopulations. The bar chart on the left shows the number of two haplotypes in distinct countries. The map in the middle displays the ratio of two haplotypes in the different provinces of China. The column diagrams below represent the number of two haplotypes in different subpopulations. (f) Expression of *GbLP1* in high-lint-percentage accession Ashi (haplotype G) and low-lint-percentage accession XH33 (haplotype C) at fibre developmental stages (0, 5, 10, 15, 20, 25 DPA), detected by RNA-seq (FPKM value). Data are average values with standard deviation ($n = 3$ varieties with three technical repeats). Single (*), double (**) and triple (***) asterisks mark statistical significance levels of $P < 0.05$, 0.01 and 0.001 respectively. (g) qRT-PCR analysis of *GbLP1* expression. Wild type: WT. Transgenic lines with empty VIGS vector: pCLCrVA. Transgenic lines with target gene *GbDLP1*: pCLCrVA-*LP1*. The high-lint-percentage accession is Giza81, and low-lint-percentage accession is C352. The gene expression level for low-lint-percentage accession wild type (H_WT) was set to 1. *GbUBQ7* is an internal control. (h) LP phenotypic values of transgenic individuals. (i) The evolutionary origins of *GbLP1*. We built unrooted trees using the maximum likelihood method in MEGA7, based on complete CDS sequences. (j) Selective pressure analysis on homologous CDS sequences of *GbLP1*. Homologous sequence in each cotton species was represented by its genome name on the left side of the circle. The difference value (Ka-Ks) of each group of homologous comparisons was indicated in coloured rectangles according to the colour bar in the upper left corner. Two types of selection, purifying (in red) and positive (in blue), are on the right side of the circle.

same functional annotation, that is casein kinase I (Table S19). Our analysis also yielded additional, previously unrecognized loci associated with fibre quality, yield, and other traits (Table S9–S12), most of which were associated with fibre quality (followed by disease resistance, yield and maturity), and many of which were located on the chromosomes that originated in the non-lint producing parent (i.e. D03, D05, D09, D10, D11). These results were consistent with the previous reports that more loci associated with fibre quality and yield were in the Dt than in the At subgenome (Ma *et al*., 2018b).

GWAS analysis of genes potentially contributing to agronomic traits

Sea Island cotton (*Gossypium barbadense*) has superior fibre quality, but poor adaption to biotic (e.g. *Fusarium wilt* disease) and abiotic (e.g. drought and salinity) stresses, as well as low yield, which collectively limit its commercial importance. Solutions for circumventing this productivity bottleneck include improving adaptability and yield of Sea Island cotton or transferring key genes from *G. barbadense* to Upland cotton. These twin paths lend significance to the goal of mining important genes responsible for fibre quality, yield and disease resistance in Sea Island cotton.

The abundance of data generated here revealed several genes related to key fibre and disease resistance traits in Sea Island cotton, including the underlying allelic and expression variation associated with domestication. We found alleles associated with superior fibre quality (FL and FS) and resistance to *Fusarium oxysporum* (DP) that included two genes encoding RING-type zinc-finger domain-containing proteins. These proteins, that is an E3 ubiquitin ligase gene (*Gbar_A05G017500*) for FL and an ATP-dependent RNA helicase gene (*Gbar_A05G014160*) related to LP, were the members of gene families previously thought to influence fibre production. In *Arabidopsis*, the E3 ubiquitin ligase regulated asymmetric cell division and cell proliferation in the root meristem (Kinoshita *et al*., 2015a), worked downstream of the CLV signalling pathway in the shoot apical meristem (Kinoshita *et al*., 2015b) and played a part in cytokinin and developmental processes (Wang *et al*., 2017b). In Upland cotton, an ubiquitin ligase protein encoded by *GhHUB2* promoted fibre elongation by ubiquitinating and degrading *GhKNL1* via the ubiquitin-26S proteasome pathway (Feng *et al*., 2018). Another Upland cotton gene (*GhRING1*) encoding a RING-type ubiquitin ligase (E3) protein had high expression in the early stages of fibre development, and the expression of the promoter of its *Arabidopsis* homolog, At3g19950, was activated in trichomes (Ho *et al*., 2010). Recently, another GWAS analysis using Sea Island cotton identified an E3 ubiquitin-protein ligase gene *GB_A03G0335* associated with fibre quality measures (Fang *et al*., 2021). Together, these studies supported the potential role of *GbFL2* as an E3 ubiquitin-protein ligase contributing to fibre quality. The role for the other one, that is the ATP-dependent RNA helicase gene *GbLP1* (*Gbar_A05G014160*), in fibre production was less clear; however, salinity stress suppressed ATP-dependent RNA helicase expression, which also reduced lint percentage (Gong *et al*., 2017). Because higher expression of *GbLP1* was associated with increased lint production, this implied an indirect association between ATP-dependent RNA helicase and cotton lint percentage.

For fibre strength, we identified the candidate gene *GbFS1*, which encoded a Casein kinase I, a multifunctional protein kinase with serine/threonine protein kinase active sites (Gross and Anderson, 1998). In rice, casein kinase I phosphorylated the DELLA protein SLR1, stabilized SLR1 and negatively regulated gibberellic acid (GA) signalling (Dai and Xue, 2010). In Upland cotton, exogenously applied gibberellic acid (GA_3) improved fibre strength in natural-coloured cottons (Zhang *et al*., 2017). GA promoted secondary cell wall development in cotton fibre cells by regulating expression of sucrose synthase genes (Xiao *et al*., 2019). We inferred that *GbFS1* might regulate fibre strength via the gibberellic acid signalling pathway in Sea Island cotton.

We also detected two genes, *GbDP1* and *GbDP2*, both on the D03 chromosome that appeared to have the role in resistance to *Fusarium wilt* disease. Recently, another newly identified gene (*Gh_D03G0209)* on D03 of Upland cotton was shown to affect resistance to FOV (Liu *et al*., 2021). It may be that the disease resistance networks are diverse, because *Gh_D03G0209* encoded a GLUTAMATE RECEPTOR-LIKE (GLR) protein, whereas *GbDP1* encoded a Zinc-finger homeodomain protein 6 (ZHD6). Alternatively, these proteins operated on different aspects of the same

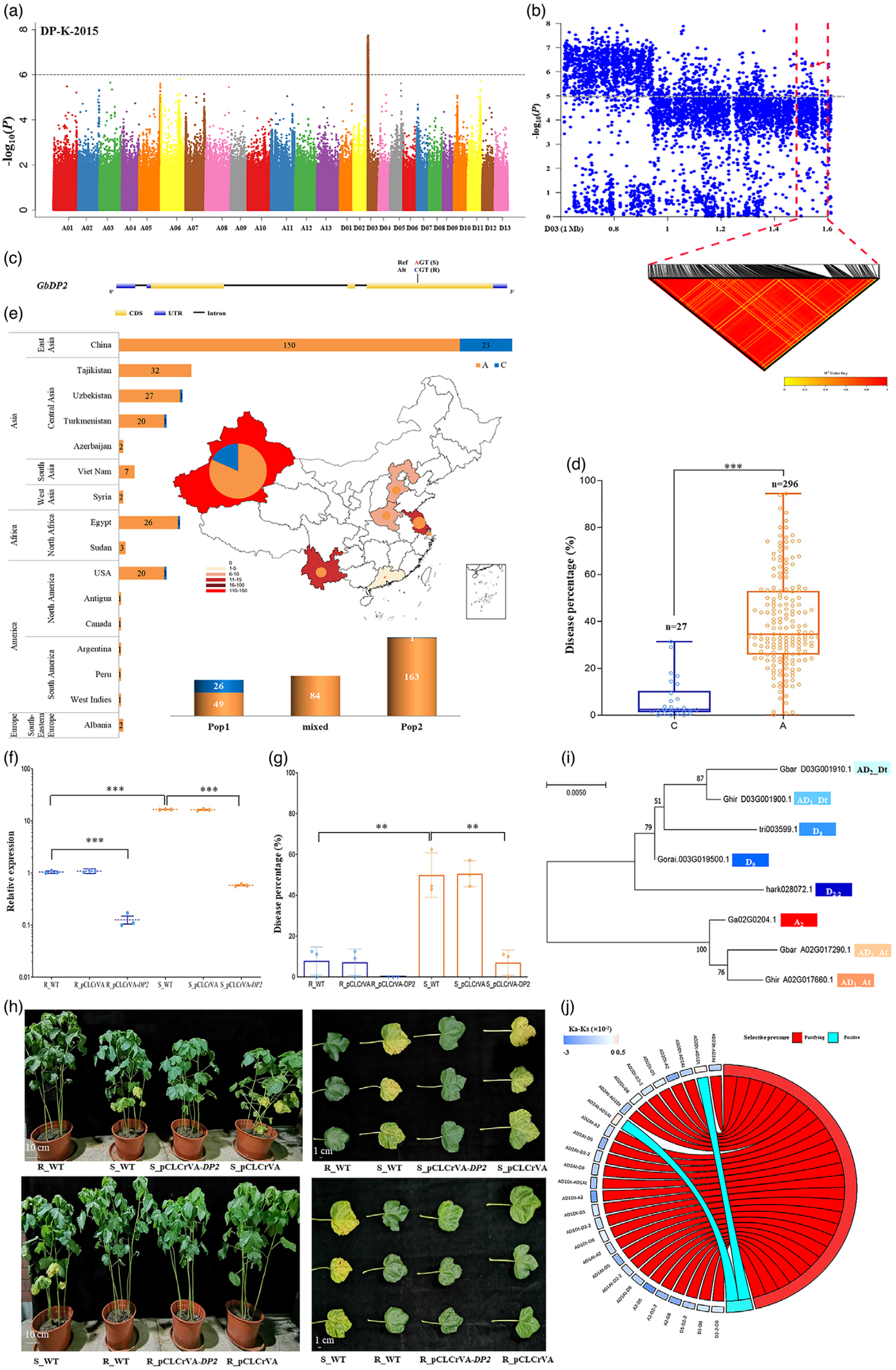
(a)
DP-K-2015
-log10(P)
A01 A02 A03 A04 A05 A06 A07 A08 A09 A10 A11 A12 A13 D01 D02 D03 D04 D05 D06 D07 D08 D09 D10 D11 D12 D13
(b)
-log10(P)
D03 (1 Mb) 0.8 1 1.2 1.4 1.6
R² Color Key
(c)
GbDP2
Ref AGT (S)
Alt CGT (R)
5' 3'
CDS UTR Intron
(e)
East Asia China 150 23
Asia Central Asia Tajikistan 32
Uzbekistan 27
Turkmenistan 20
Azerbaijan 2
South Asia Viet Nam 7
West Asia Syria 2
Africa North Africa Egypt 26
Sudan 3
America North America USA 20
Antigua 1
Canada 1
South America Argentina 1
Peru 1
West Indies 1
Europe South-Eastern Europe Albania 2
A C
0 1-5 6-10 11-15 16-100 110-150
26 49 Pop1
84 mixed
1 163 Pop2
(d)
Disease percentage (%)
***
n=27
n=296
C A
(f)
Relative expression
***
***
***
R_WT R_pCLCrVA R_pCLCrVA-DP2 S_WT S_pCLCrVA S_pCLCrVA-DP2
(g)
Disease percentage (%)
**
**
R_WT R_pCLCrVA R_pCLCrVA-DP2 S_WT S_pCLCrVA S_pCLCrVA-DP2
(i)
0.0050
87 51 79 100 76
Gbar D03G001910.1 AD2_Dt
Ghir D03G001900.1 AD1_Dt
tri003599.1 D8
Gorai.003G019500.1 D5
hark028072.1 D2-2
Ga02G0204.1 A2
Gbar A02G017290.1 AD2_At
Ghir A02G017660.1 AD1_At
(h)
10 cm
R_WT S_WT S_pCLCrVA-DP2 S_pCLCrVA
1 cm
R_WT S_WT S_pCLCrVA-DP2 S_pCLCrVA
10 cm
S_WT R_WT R_pCLCrVA-DP2 R_pCLCrVA
1 cm
S_WT R_WT R_pCLCrVA-DP2 R_pCLCrVA
(j)
Ka-Ks (×10⁻²)
-3 0 0.5
Selective pressure Purifying Positive

Figure 4 Identification of the DP causal gene *GbDP2* on chromosome Dt03. (a) Manhattan plot for DP. Dashed line represents the significance threshold (-$\log_{10}P = 6$). Effect values of genetic markers were tested using *F* tests and corrected for multiple testing using Bonferroni correction. (b) Local Manhattan plot (top) and LD heatmap (bottom) surrounding the peak on Dt03. Dashed line represents the significance threshold (-$\log_{10}P = 5$). We used an F test to perform statistical analysis. Red arrows mark the positions of the nonsynonymous SNP D03_1537617, which is located within *Gbar_D03G001910* (*GbDP2*). Red dotted lines mark the candidate region. (c) Structure of gene *GbDP2*. Blue and yellow rectangles mark UTR and CDS respectively. (d) Box plot for DP, based on the haplotypes of the two SNPs. In the box plots, the centre line indicates the median, box limits are the upper and lower quartiles, and whiskers mark the range of the data. *n* denotes the number of accessions with the same genotype. We use a two-tailed *t*-test to perform the significance analysis. (e) Haplotype distribution in diverse geographical regions and subpopulations. The bar chart at the left shows the number of two haplotypes in distinct countries. The map in the middle displays the ratio of two haplotypes in the different provinces of China. The column diagrams below represent the number of two haplotypes in different subpopulations. (f) qRT-PCR analysis of *GbDP2* expression in leaves after fusarium inoculation in highly resistant (R) accession (XH42) and highly susceptible (S) accession (Su7871-). We set the gene expression level from the highly resistant (R) accession as 1. *GbUBQ7* is an internal control. Data are average values with standard deviation ($n = 3$ varieties with three technical repeats). Single (*), double (**) and triple (***) asterisks mark statistical significance levels of $P < 0.05$, 0.01 and 0.001 respectively. (g) Disease percentage of R_WT, S_WT, S_pCLCrVA-*DP2* and S_pCLCrVA plants at 25 d post-inoculation (dpi) with FOV. (h) VIGS phenotypes of *GbDP2* in highly resistant (R) accession (XH42) and highly susceptible (S) accession Su7871- after inoculation with FOV. Wild type of highly resistant (R) accession XH42 (R_WT) and highly susceptible (S) accession Su7871- transformed with empty VIGS vector (S_pCLCrVA) were used as controls. The leaves in the right panel were obtained from the individual plants in the left panel. (i) The evolutionary origins of *GbDP2*. We built unrooted trees using the maximum likelihood method in MEGA7, based on complete CDS sequences. (j) Selective pressure analysis on homologous CDS sequences of *GbDP2*. Homologous sequence in each cotton species is represented by its genome name on the left side of the circle. The difference value (Ka-Ks) of each group of homologous comparisons is indicated by coloured rectangles according to the colour bar in the upper left corner. Two types of selection, purifying (in red) and positive (in blue), are on the right side of the circle.

network. Zinc-finger homeodomain (ZF-HD) subfamily proteins played specific roles in pathogen signalling and plant defences by activating *CaM4* gene expression in response to pathogens (Park *et al.*, 2007). The other defence gene, *GbDP2*, encoded a wall-associated receptor kinase-like 14 (WAKL14). Many *WAKL* genes were correlated with plant resistance and immune responses. For instance, *CsWAKL08*, a pathogen-induced wall-associated receptor-like kinase in sweet orange, conferred resistance to citrus bacterial canker via ROS control and JA signalling (Li *et al.*, 2020). OsWAKL21.2 activated rice immune responses by its kinase activity and *Arabidopsis* immune responses by its guanylate cyclase activity (Malukani and Ranjan 2020). Although the precise function of our five candidate genes identified here remains unclear, we confirmed their influences on their respective phenotypes using VIGS transgenic experiments in Sea Island cotton here.

Cotton improvement by GWAS and pedigree analysis

Modern Sea Island cotton cultivars principally were derived from three gene pools: Egyptian type, American type and Middle-Asian type (Abdullaev *et al.*, 2017). In Xinjiang, Sea Island cotton varieties were derived from five backbone parents of Central Asia, including 2И3, C6022, 8763И, 5230Ф and 9122И. JH1, a variant with the early maturity of 9122И, was the core germplasm source used to produce more than 50 varieties, including at least 10 main cultivars. Here, we extracted a pedigree composed of 19 varieties, including 9122И and JH1 that were involved in developing the cultivar XH39, which has early maturity, high resistance and superb fibre quality. Our analyses revealed a dN/dS ratio and blocks of low diversity consistent with strong directional selection. The total size and gene number in the low diversity regions were biased towards the Dt subgenomes, supporting the notion that selection for fibre improvement has been asymmetric across genomes (Ma *et al.*, 2019; Wang *et al.*, 2017a).

In Upland cotton, pedigree-based genome resequencing has been an effective tool for researchers to detect candidate genes related to important traits via genetic transmission analysis (Fang *et al.*, 2017; Lu *et al.*, 2019; Ma *et al.*, 2019). In our pedigree, XH39 and its related accession XH60 exhibited divergent improvement trends, with the former focused on fibre quality (FL and FS), while the latter targeted yield (LP and SI). This divergence in selection might predict different targeted genes, but we found some common genes underlying traits of the same category, for example FL/FS, LP and SI. While the genes in some categories, for example GP and DP, likely had no influence on fibre quality or yield, it is possible that some could simultaneously regulated fibre quality (i.e. FS), or yield (i.e. LP, BN) and growth period.

In summary, here we provided a detailed depiction of the Chinese Sea Island cotton gene pool, describing diversity and phylogenetic and population structure. We generated a WGS dataset for the community and demonstrated its utility via a comprehensive GWAS analysis. We further described the inferences of candidate genes to facilitate molecular-marker selection and genetic improvement for great disease resistance, superb fibre quality and high yield of cotton. Pedigree analysis of XH39 and XH60 provided evidences for the basis of increased fibre quality and yield, as well as the improvement to *Fusarium wilt* disease resistance. Our research laid a foundation for understanding polymorphism in Chinese Sea Island cotton, as well as introgression from other sources and artificial selection. In addition, the key genes identified here for fibre quality, yield and disease resistance can be further explored, for example, to decipher their participations in regulatory networks and the genotype-to-phenotype connections. Elite Chinese Sea Island varieties with excellent haplotype combinations have great agronomic potential for cotton improvement. The present study put forward a significant step to the exploration, understanding and utilization of the broad gene pool.

Methods

Sampling

We collected 336 *G. barbadense* accessions (including 19 accessions in pedigree analysis) derived from major global cotton-growing countries from seed stocks maintained at China Agricultural University, Beijing. The original diversity was evaluated based on their geographical distribution and breeding history. The geographic origins of these accessions included the major cotton-growing countries, that is China (Northwest Inland Region, Yellow River Basin, Yangtze River Basin, Southwest and

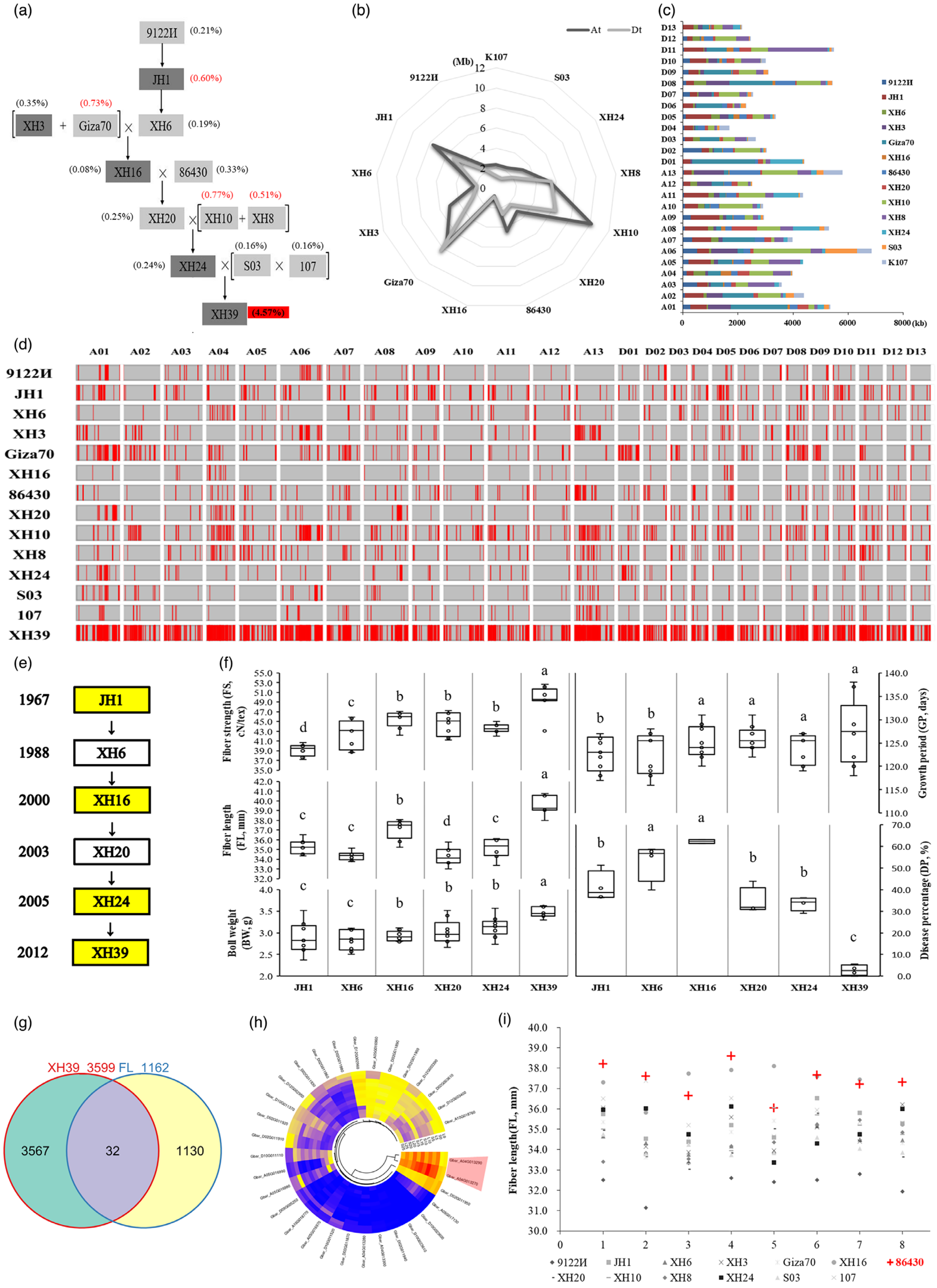
(a)
9122И (0.21%)
JH1 (0.60%)
XH3 (0.35%) + Giza70 (0.73%) × XH6 (0.19%)
XH16 (0.08%) × 86430 (0.33%)
XH20 (0.25%) × XH10 (0.77%) + XH8 (0.51%)
XH24 (0.24%) × S03 (0.16%) × 107 (0.16%)
XH39 (4.57%)
(b)
At
Dt
(Mb)
K107
S03
XH24
XH8
XH10
XH20
86430
XH16
Giza70
XH3
XH6
JH1
9122И
(c)
D13 D12 D11 D10 D09 D08 D07 D06 D05 D04 D03 D02 D01 A13 A12 A11 A10 A09 A08 A07 A06 A05 A04 A03 A02 A01
0 2000 4000 6000 8000 (kb)
9122И JH1 XH6 XH3 Giza70 XH16 86430 XH20 XH10 XH8 XH24 S03 K107
(d)
A01 A02 A03 A04 A05 A06 A07 A08 A09 A10 A11 A12 A13 D01 D02 D03 D04 D05 D06 D07 D08 D09 D10 D11 D12 D13
9122И JH1 XH6 XH3 Giza70 XH16 86430 XH20 XH10 XH8 XH24 S03 107 XH39
(e)
1967 JH1
1988 XH6
2000 XH16
2003 XH20
2005 XH24
2012 XH39
(f)
Fiber strength (FS, cN/tex)
Fiber length (FL, mm)
Boll weight (BW, g)
Growth period (GP, days)
Disease percentage (DP, %)
JH1 XH6 XH16 XH20 XH24 XH39
d c b b b a
c c b d c a
c c b b b a
b b a a a a
b a a b b c
(g)
XH39_3599 FL_1162
3567 32 1130
(h)
(i)
Fiber length(FL, mm)
9122И JH1 XH6 XH3 Giza70 XH16 86430
XH20 XH10 XH8 XH24 S03 107

Figure 5 Pedigrees and genomic constitution of Sea Island cotton cultivar XH39. (a) A pedigree of XH39, including 13 parental varieties. We marked the main cultivars in the dark-grey background. (b) Total length of genomic fragments inherited from 13 parents to XH39 in At and Dt subgenome. The genetic constitutions in At and Dt subgenome are in dark and light grey respectively. (c) Accumulated length of genetic fragments inherited from 13 parents to XH39 on 26 chromosomes. (d) Homologous fragments of XH39 in 13 related parents of the pedigree. 13 parents are along the vertical axis (left). The horizontal axis (top) marks different chromosomes, A01-D13. Unique genetic segments passed from each parent to XH9 according to the genetic pathway shown in Fig 5a. Aligned sequences are highlighted in red to show their proportional physical location, and unaligned segments are indicted in grey box. (e) The simplified pedigree of XH39, including six critical direct-systematic-breeding varieties in chronological order on the left. Here, four main cultivars are in the bright-yellow background. (f) Statistical analysis of five traits in six varieties in the simplified pedigree of XH39. The phenotypic values were from different environments (n = 8, 8, 9, 9 and 4 for FL, FS, BW, GP and DP). We used the least significant difference (LSD) method in one-way ANOVA, *p*-value<0.05. Boxes span from the first to the third quartiles. The centre lines represent the median values, and the whiskers show data that lie within the 1.5 interquartile ranges of the lower and upper quartiles. The small hollow circles represent the outliers of the phenotypic data in different environments. (g) Venn diagram showing the overlapping FL-related genes (in middle purple) in the genetic transmission and GWAS analyses. (h) Circular heatmap showing expression differences of 32 overlapping FL-controlling genes in 0, 5, 10, 15, 20 and 25 DPA fibres of FL extreme lines. Two genes, *Gbar_A04G013270* and *Gbar_A04G013290*, with the highest expression in 5-25DPA fibre, are in the red trapezoid. (i) Fibre length of 13 parental lines of XH39. 1-8 on the horizontal axis represent eight original environments, including Awat-2018, Awat-2019, Baotou lake-2019, Korla-2013, Korla-2015, Korla-2016, Korla-2018 and Korla-2019. Parental origin of two high-expression genes (in Figure 5h) in XH39 was 86430 (highlighted in red).

South China), the United States, the former Soviet Union (Uzbekistan, Tajikistan, Turkmenistan and Azerbaijan), Viet Nam, Syria, Antigua, Argentina, West Indies, Peru, Albania, Egypt and Sudan (Figure S1 and Table S1). Additionally, we had seven pair of samples that were initially bred from the same varieties, but they were not exactly genetically identical, because they came from the different lines, so they were not sample duplication in terms of genomic composition (Su *et al.*, 2020); therefore, we labelled the source as cultivars/lines in Table S1.

Planting and phenotyping

Phenotyping of 15 traits was performed across four locations over six years (not four locations × six years, the detailed is in the next paragraph). Three locations were comprised of Yacheng in Hainan (H) Province (Southern China), and Korla (K) and Awat (A) in Xinjiang (Northwest Inland; Table S8). All accessions were planted in an experimental field with an arrangement-order design, including two replicates. Each plot at the H-site contained one row 4 m in length, 11–13 plants per row, ~33 cm between plants within each row and 75 cm between rows. Plot specifications at K and A locations contained 18–20 plants per row 2 m in length, ~11 cm between plants within each row and 66 cm between rows. Cotton was sown in mid-to-late April and was harvested in mid-to-late October in the Xinjiang locations, whereas the cotton was sown in mid-to-late October and was harvested in mid-to-late April in Hainan.

We characterized 15 traits and obtained a total of 119 sets of phenotypes. Nine traits (FL, FS, FM, FU, FE, FBN, BN, SBW, LP, GP, FNFB and PH) were recorded in nine locations×years sets (Table S9). SI, DP and FBT were assessed in six, four and one environment respectively (Table S9). Twenty naturally opened bolls were hand-harvested to calculate the SBW (g) and gin the fibres. SI was obtained after counting and weighing 100 cotton seeds. Fibre samples were separately weighed to calculate LP. Fibre samples were evaluated for quality traits with a high-volume instrument (HFT9000) at the Ministry of Agriculture Cotton Quality Supervision, Inspection and Testing Center in China Colored Cotton Group Corporation, Urumqi, China. Data were collected on the fibre upper-half mean length (FL, mm), FS (cN/tex), FM, FE (%) and FU (%).

DNA isolation and genome resequencing

The leaves from a single plant of each accession were sampled and used for DNA extraction. Total genomic DNA was extracted with a Plant DNA Mini Kit (Cat # DN1502, Aidlab Biotechnologies, Ltd.), and 350-bp whole-genome libraries were constructed for each accession by random DNA fragmentation (350 bp), terminal repair, PolyA tail addition, sequencing connector addition, purification, PCR amplification and other steps (TruSeq Library Construction Kit, Illumina Scientific Co., Ltd., Beijing, China). Subsequently, we used the Illumina HiSeq PE150 platform to generate 9.78 Tb raw sequences with 150 bp read length.

Sequencing reads quality checking and filtering

To avoid reads with artificial bias (i.e. low-quality paired reads, which primarily result from base-calling duplicates and adaptor contamination), we removed the following types of reads: (i) reads with ≥10% unidentified nucleotides (N); (ii) reads with adaptor sequences; (iii) reads with >50% bases having Phred quality Q ≤ 5. Consequently, 9.42 Tb high-quality sequences were used in subsequent analyses (Table S1).

Sequencing reads alignment

The remaining high-quality reads were aligned to the genome of *G. barbadense* 3–79 (http://cotton.hzau.edu.cn/EN/download.php; Wang *et al.*, 2019) with BWA software (version: 0.7.8) with the command 'mem -t 4 -k 32 -M'. BAM alignment files were subsequently generated in SAMTOOLS v.1.4 (Li *et al.*, 2009), and duplications were removed with the command 'samtools rmdup'. Additionally, we improved the alignment performance through (i) filtering the alignment reads with mismatches≤5 and mapping quality = 0 and (ii) removing potential PCR duplications. If multiple read pairs had identical external coordinates, only the pairs with the highest mapping quality were retained.

Population SNP detection

After alignment, SNP calling on a population scale was performed with the Genome Analysis Toolkit (GATK, version v3.1) with the UnifiedGenotyper method (McKenna *et al.*, 2010). To exclude SNP-calling errors caused by incorrect mapping, only high-quality SNPs (depth ≥ 4 (1/3 of the average depth), map quality ≥20, the missing ratio of samples within the population ≤ of 10% (3,487,043 SNPs) or of 20% (4 052 759 SNPs), and minor allele frequency (MAF) >0.05) were retained for subsequent analyses. SNPs with the missing ratio ≤ of 10% were used in PCA/phylogenetic tree/structure analyses, whereas

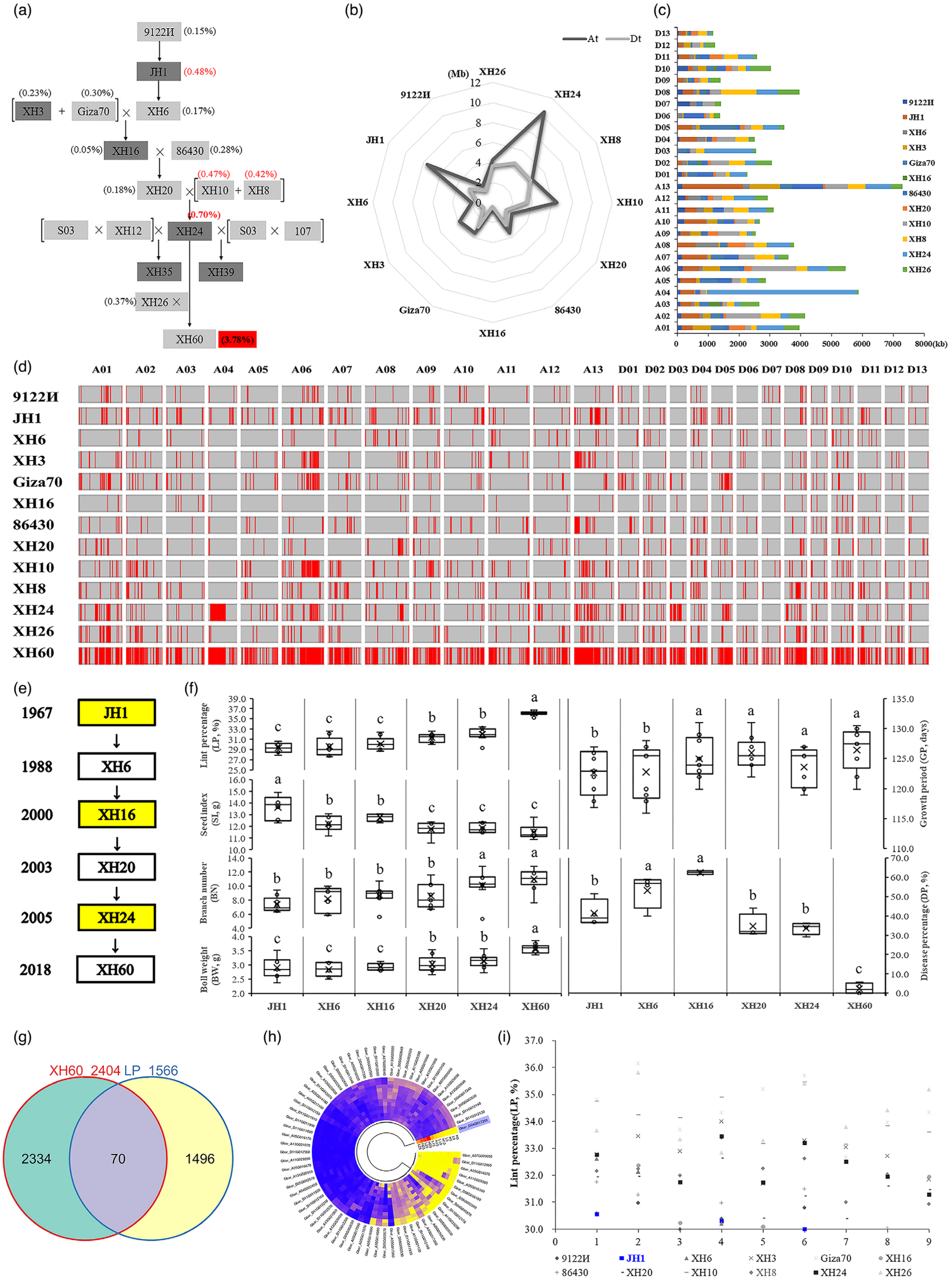
(a)
9122И (0.15%)
JH1 (0.48%)
(0.23%) XH3 + (0.30%) Giza70 × XH6 (0.17%)
(0.05%) XH16 × 86430 (0.28%)
(0.18%) XH20 × (0.47%) XH10 + (0.42%) XH8
(0.70%)
S03 × XH12 × XH24 × S03 × 107
XH35
XH39
(0.37%) XH26 ×
XH60 (3.78%)
(b)
At
Dt
(Mb) 12 10 8 6 4 2 0
XH26 XH24 XH8 XH10 XH20 86430 XH16 Giza70 XH3 XH6 JH1 9122И
(c)
D13 D12 D11 D10 D09 D08 D07 D06 D05 D04 D03 D02 D01 A13 A12 A11 A10 A09 A08 A07 A06 A05 A04 A03 A02 A01
0 1000 2000 3000 4000 5000 6000 7000 8000(kb)
9122И JH1 XH6 XH3 Giza70 XH16 86430 XH20 XH10 XH8 XH24 XH26
(d)
A01 A02 A03 A04 A05 A06 A07 A08 A09 A10 A11 A12 A13 D01 D02 D03 D04 D05 D06 D07 D08 D09 D10 D11 D12 D13
9122И JH1 XH6 XH3 Giza70 XH16 86430 XH20 XH10 XH8 XH24 XH26 XH60
(e)
1967 JH1
1988 XH6
2000 XH16
2003 XH20
2005 XH24
2018 XH60
(f)
Lint percentage (LP, %)
Seed index (SI, g)
Branch number (BN)
Boll weight (BW, g)
Growth period (GP, days)
Disease percentage (DP, %)
JH1 XH6 XH16 XH20 XH24 XH60
(g)
XH60 2404 LP 1566
2334 70 1496
(h)
(i)
Lint percentage(LP, %)
37.0 36.0 35.0 34.0 33.0 32.0 31.0 30.0
0 1 2 3 4 5 6 7 8 9
9122И JH1 XH6 XH3 Giza70 XH16
86430 XH20 XH10 XH8 XH24 XH26

Figure 6 Pedigrees and genomic constitution of Sea Island cotton cultivar XH60. (a) A pedigree of XH60 including 12 parental varieties. Main cultivars are marked in dark-grey background. (b) Total length of genomic fragments inherited from 12 parents in the At and Dt subgenome. Length of genetic components in At and Dt subgenome is indicated in dark and light grey respectively. (c) Accumulated length of genomic fragments inherited from 12 parents on 26 chromosomes. (d) Homologous fragments of XH60 in 12 related parents of the pedigree (listed on the vertical axis (left)). The horizontal axis (top) indicates different chromosomes. Unique genetic segments in each parent are specifically passed to XH60 according to the genetic pathway shown on Fig 6a. Aligned sequences are highlighted in red to show their proportional physical location, and unaligned segments are indicted in grey box. (e) Simplified pedigree of XH60 with four main cultivars highlighted in light yellow. (f) Statistical analysis of lint percentage (LP, %), seed index (SI, g), boll weight (BW, g), growth period (GP, days) and disease percentage (DP, %) of six varieties in the simplified pedigree of XH60 using their phenotypic values from different environments (n = 9, 9, 9, 9 and 4 for LP, SI, BW, GP and DP), though least significant difference (LSD) method in one-way ANOVA analysis. P-value < 0.05. Boxes span the first to third quartiles, centre lines represent median values, and whiskers show data within the 1.5 interquartile ranges of the lower and upper quartiles. The small hollow circles represent phenotypic outliers. (g) Venn diagram showing the overlapping LP genes (in middle purple) obtained by genetic transmission analysis and GWAS analysis. (h) Circular heat map illustrating expression differences of 70 overlapping LP genes in 0, 5, 10, 15, 20 and 25 DPA fibres of LP extreme lines. The gene, *Gbar_D04G017350*, with the highest expression in 5-25DPA fibre, is highlighted in the blue rectangle. (i) Lint percentage of 13 parental lines of XH60. 1-9 on the horizontal axis represent nine original environments, including Awat-2018, Awat-2019, Baotou lake-2019, Korla-2013, Korla-2014, Korla-2015, Korla-2016, Korla-2018 and Korla-2019. JH1 in blue was the parental origin of the high-expression genes (in Figure 6h) in XH60.

SNPs with a missing ratio ≤ of 20% were used in the rest of the analyses.

Annotation of genetic variants

SNP annotation was performed according to the *G. barbadense* reference genome using the package ANNOVAR v1.0.0 (Wang *et al*., 2010). Based on the genome annotation, SNPs were categorized in exonic regions (overlapping a coding exon), intronic regions (overlapping an intron), splicing sites (within 2 bp of a splicing junction), upstream or downstream regions (within a 1 kb region upstream from the transcription start site or downstream from the transcription stop site), intergenic regions, transitions (ts), transversions (tv) and ts/tv. SNPs in exonic regions were further grouped into stop gain and stop loss (SNPs causing the gain and loss of stop codons), synonymous SNPs (those did not cause amino acid changes) and nonsynonymous SNPs (those caused amino acid changes).

Phylogenetic and population structure analyses

To clarify phylogenetic relationships from a genome-wide perspective, an individual-based NJ (neighbour-joining) tree was constructed using *P* distance in TreeBestv1.9.2 software (http://treesoft.sourceforge.net/treebest.shtmcl). Bootstrap values were derived from 1000 resampling. Population genetic structure was assessed using the software Admixture (1.23). The number of assumed genetic clusters *K* ranged from 2 to 7, with 10 000 iterations for each run. We also conducted PCA to evaluate the genetic structure in GCTA 1.24.2 (http://cnsgenomics.com/software/gcta/pca.html) software (Li and Durbin, 2010). The significance level of the eigenvector was determined with the Tracy-Widom test.

Population genetic analysis

Fixation statistics (F_{ST}) and nucleotide diversity (θ_π) were calculated in VCFtools v0.1.15 (Danecek *et al*., 2011), with sliding windows of 10 kb.

Linkage-disequilibrium analysis

The software Plink v1.07 (Purcell *et al*., 2007) was used to calculate the LD coefficient (r^2) between pairwise high-quality SNPs; the parameters were set as: '--1d-window-r2 0 --ld-window 99999 --ld-window-kb 1000', and the results were used to estimate LD decay.

GWAS analysis

Totally, 4 052 759 SNPs (MAF > 0.05; Quality ≥ 20; GQ ≥ 5; missing rate ≤ 0.2; depth ≥ 4) were used in GWAS for the 15 different traits. To correct for the effect of accession imbalance based on the geographical distribution, association analysis was conducted with the genome-wide efficient mixed-model association (GEMMA 0.94.1, http://www.xzlab.org/software.html) software package (Zhou and Stephens, 2012). For mixed-linear model analysis, we used the following equation:

$$y = \mathrm{X}\alpha + \mathrm{S}\beta + \mathrm{K}\mu + \mathbf{e}$$

where y represents phenotype; α and β are fixed effects representing marker effects and non-marker effects respectively; and μ represents unknown random effects. X, S and K are the incidence matrices for α, β and μ, respectively, and **e** is a vector of random residual effects. Additionally, the top three PCs were used to build up the S matrix for population structure correction, and the matrix of simple matching coefficients was used to build up the K matrix. The analyses were performed in the GEMMA software package. The parameters were set as: 'gemma -bfile file -k kinship -lmm 1 -o outfile -miss 0.2 -maf 0.05 -c covariates (GCTA: PCA)'. The effect values of our genetic markers were tested by *F* tests and corrected for multiple testing using Bonferroni correction. Only the most obvious SNP peak in Manhattan plot was chosen as the candidate SNP. Meanwhile, to estimate the difference between observed and predicted values of quantitative traits, all Manhattan results were validated by Q-Q plots.

Estimating breeding value

BLUP (Poland *et al*., 2011) was used to calculate the breeding values with lme4 packages in R (version 3.5.3). The formula was as follows:

$$Y = \mu + \mathrm{Line} + \mathrm{Loc} + \mathrm{Year} + (\mathrm{Rep\ in\ Loc} \times \mathrm{Year}) + (\mathrm{Line} \times \mathrm{Loc}) + (\mathrm{Line} \times \mathrm{Year}) + \epsilon$$

where Y, μ, Line and Loc represent phenotype, intercept, variety effects and environmental effects respectively. Rep indicates different repetitions, and ε represents random effects. Rep in Loc × Year shows the interaction between repetition in the same location and year. Line × Loc is used to display the interaction between variety and environment. Line × Year is used to display the interaction between variety and year.

Transcriptome sequencing

Five Sea Island cotton extreme accessions were planted in the field in 2019 (Table S21). Bolls were collected during the initiation stage (0 DPA), cell elongation stage (5, 10, 15 DPA) and secondary-wall synthesis stage (20, 25 DPA). Total RNA was extracted from the fibres of the boll samples with an EASYspin RNA Plant Mini Kit (Cat # RN0902, Aidlab Biotechnologies., Ltd). The qualified RNA treated with DNase I (Takara Biomedical Technology Co., Ltd., Beijing, China) was used for constructing cDNA library, HiSeq sequencing, assembling, mapping (HISAT 2.0.4 (Kim *et al.*, 2015), with default parameters), analysing gene expression (HTSeq v0.6.1, -m union; Anders *et al.*, 2015), detecting SNP (GATK v3.5, QUAL < 30.0 & QD < 5.0; McKenna *et al.*, 2010), identifying differentially expressed genes (DESeq 1.10.1, $P_{adj} < 0.05$; Anders and Huber, 2010), GO (GOSeq, Release2.12, Corrected *P*-value < 0.05; Young *et al.*, 2010) and KEGG (KOBAS v2.0, Corrected *P*-value < 0.05; Mao *et al.*, 2005) annotation according to the method in our laboratory (Shi *et al.*, 2015).

Functional characterization of *GbDP1/2* genes

Sea Island cotton (*Gossypium barbadense*) highly susceptible (S) accession 15-3464 and highly resistant (R) accession T10-280 were used for VIGS transformation of *GbDP1*. Sea Island cotton highly resistant (R) accession (XH42) and highly susceptible (S) accession Su7871- were used for VIGS transformation of *GbDP2*. For virus-induced gene silencing (VIGS), 516-bp and 502-bp fragments from *GbDP1* and *GbDP2* were separately cloned into the *Pac*I and *Spe*I sites of the pCLCrV-VA vector (primers used in Table S20). To analyse expression and silencing efficiency of *GbDP1/2*, leaves were harvested at 25 days post-inoculation (dpi) with FOV in two sets of resistant and susceptible wild-type (R_WT and S_WT) accessions, their *DP*-transgenic accession (S_pCLCrVA-*DP1*, S_pCLCrVA-*DP2*, R_pCLCrVA-*DP1* and R_pCLCrVA-*DP2*) and empty-vector transformants (S_pCLCrVA and R_pCLCrVA). Total RNA (~2 μg) was extracted and was then reverse-transcribed in a 20 μL reaction mixture with PrimeScript™ RT reagent Kit with gDNA Eraser (Perfect Real Time) (Cat # RR047A; Takara). 1 μL sample aliquots were used as templates for qRT-PCR analysis. Three technical replicates per sample and three biological-replicate samples were analysed for each experiment. *UBQ7* was used as the internal control for qRT-PCR data analysis.

VIGS experiments of *GbFL2*, *GbFS1* and *GbLP1*

Sea Island cotton long-fibre accession XH58 and short-fibre accession Ashi were used for VIGS transformation receptors *GbFL2*. Sea Island cotton high-fibre-strength accession XH37 and low-fibre-strength accession LuoSaiNa were used for VIGS transformation receptors *GbFS1* respectively. Sea Island cotton high-lint-percentage accession Giza81 and low-lint-percentage accession C352 were used for VIGS transformation receptors *GbLP1*. For the VIGS experiments, plants were grown on the field of Hainan for 1 growing season. Inserts to generate pCLCrVA-*FL2/FS1/LP1,* approximately 500-bp fragments, were amplified from *G. barbadense* cDNA. Primer pairs to generate pCLCrVA-*FL2/FS1/LP1* vectors are shown in Table S20. PCR fragments were cloned into the pCLCrVA plasmid using *Pac*I and *Spe*IC. Plasmids pCLCrVB, pCLCrVA, and their derivatives were transformed into *A. tumefaciens* GV3101 (Shanghai Weidi Biotechnology Co., Ltd, Shanghai, China) using its supplied method. Before transformation, *Agrobacterium* containing pCLCrVA or one of its derivatives were mixed with an equal volume of *Agrobacterium* containing pCLCrVB (Gu *et al.*, 2014). Mixed *Agrobacterium* solutions were infiltrated into the abaxial side of cotyledons of 2-week-old cotton seedlings using a needleless syringe as described previously (Gao *et al.*, 2013). For 4-week-old cotton seedlings, *Agrobacterium* solutions were infiltrated into the abaxial side of cotyledons and leaves together with injection into the apical growth point of stems using a bevelled needle. Two months after infiltration, RNA was extracted from cotton leaves to measure the expression of the target genes using qRT-PCR. There were 100 individual plants for each treatment. All harvested plants were used for phenotyping of LP, but for FL and FS, we chose 10 positive individuals determined by qRT-PCR for phenotyping. Statistics of significance were carried out using two-tailed t tests.

Hierarchical filtering strategy of associated SNPs/genes, QTL, candidate/key genes

Significant SNPs were screened by the criterion (-log(*P*-value) > 6). QTLs were defined according to the position of significant SNPs and the size of LD interval. In order to avoid missing key candidate genes, we defined the total size of QTL as 1Mb according to the criterion in Fang *et al.* (2017), namely, 500 kb upstream and downstream of associated SNPs, slightly larger than the size of actual LD interval (388 kb). That is, one significant SNP corresponds to 1Mb QTL interval. All genes in those QTL intervals were regarded initially as associated genes. These were filtered as follows: First, only the top three highest peak SNPs and the significant SNPs that could be repeatedly detected in at least two environments were regarded as key SNPs, thus narrowing the candidate SNPs from dozens to about 10. Second, only the genes closest to these key SNPs, at the same time having large-effect variations related to phenotype change and expressed differentially in extreme accessions, were considered as candidate genes for further transgenic validation. Finally, only genes silenced by VIGS and related to the phenotypes in question were deemed to be key genes (Figure S23).

Genetic transmission analysis

To detect genetically transmitted regions in a pedigree, we calculated the SNP ratio between parental accessions and XH39/XH60. A window size of 200 SNPs, with a step size of 20 SNPs, was used to perform genomic scans (Fang *et al.*, 2017; Jiao *et al.*, 2012). A window with the same SNP ratio ≥99% was considered as an inheritable fragment in the pedigree (Ma *et al.*, 2019). We used our Sea Island cotton fibre transcriptome data to validate the function of candidate genes.

Acknowledgements

We thank K. W. and F. L., Institute of Cotton Research, China Academy of Agricultural Sciences, for providing seeds of 86 accessions. We thank X. Y., CAU for guidance in GWAS analysis. We thank H.L., B.Z, M.Z., Z.Z. and Y.W. for their helps in functional validation. This work was supported by National Key R & D Program for Crop Breeding (2016YFD0100306) to J.H., Key Cultivation Program of Science and Technology Innovation of Xinjiang Academy of Agricultural Sciences (xjkcpy-001) to J.K., China Agriculture Research System (CARS-15-09) to A.A., Project of Agricultural Science and Technology Innovation of Shanxi Academy of Agricultural Sciences (YCX2018D2YS06) to P.L. and

Project of Modern Agricultural Science and Technology Innovation of Hebei Academy of Agriculture and Forestry Sciences (2019-3-7) to B.G.

Conflicts of interest

The authors have no conflicts of interest to declare.

Author contributions

J.H. and J.F.W. conceived and designed the research. J.K., W.W., A.A., N.Z. and J.H. prepared the population material. W.W., J.Z., M.W., L.X., J.Y., X.N., H.X., A.A. and J.K. performed field experiments and phenotyping. W.W. and N.Z. performed data integration. N.Z. performed sampling, sequencing, genomic-variant and GWAS analyses. K.J., H.N., A.G. and N.Z. performed transcriptome analyses. N.Z. and K.J. conducted gene expression analysis. J.H., N.Z., B.L., I.D., K.J. and W.W. took part in functional validation. C.C. selected the pedigree accessions and N.Z. performed pedigree analysis. Z.P., B.G., J.G., P.L., Y.S., C.C., H.N. and C.E.G. contributed to the project discussion. N.Z. and J.H. wrote the manuscript. C.E.G., J.H. and J.F.W. revised the manuscript.

Data availability statement

Raw genome resequencing reads were deposited in NCBI sequence read archive (SRA) under BioProject ID: PRJNA720817 (Table S1). VCF file with final SNPs used for GWAS analyses is available from figshare repository (https://figshare.com/articles/dataset/Sea_island_cotton_GWAS_VCFs_project/16529178). The transcriptome sequencing raw data have been submitted to the NCBI Gene Expression Omnibus (GEO) under the accession number GSE184965 (Table S21).

References

Abdullaev, A.A., Salakhutdinov, I.B., Egamberdiev, S.S., Khurshut, E.E., Rizaeva, S.M., Ulloa, M. and Abdurakhmonov, I.Y. (2017) Genetic diversity, linkage disequilibrium, and association mapping analyses of *Gossypium barbadense* L. germplasm. *PLoS One*, **12**, e0188125.

Abdurakhmonov, I.Y., Saha, S., Jenkins, J.N., Buriev, Z.T., Shermatov, S.E., Scheffler, B.E., Pepper, A.E. *et al*. (2009) Linkage disequilibrium based association mapping of fiber quality traits in *G. hirsutum* L. variety germplasm. *Genetica*, **136**, 401–417.

Anders, S. and Huber, W. (2010) Differential expression analysis for sequence count data. *Genome Biol.* **11**, R106.

Anders, S., Pyl, P.T. and Huber, W. (2015) HTSeq-a Python framework to work with high-throughput sequencing data. *Bioinformatics*, **31**, 166–169.

Cai, C., Zhu, G., Zhang, T. and Guo, W. (2017) High-density 80 K SNP array is a powerful tool for genotyping *G. hirsutum* accessions and genome analysis. *BMC Genom.* **18**, 654.

Chen, Z.J., Sreedasyam, A., Ando, A., Song, Q., De-Santiago, L.M., Hulse-Kemp, A.M., Ding, M. *et al*. (2020) Genomic diversifications of five *Gossypium* allopolyploid species and their impact on cotton improvement. *Nat. Genet.* **52**, 525–533.

Dai, C. and Xue, H.W. (2010) Rice early flowering1, a CKI, phosphorylates DELLA protein SLR1 to negatively regulate gibberellin signalling. *EMBO J.* **29**, 1916–1927.

Danecek, P., Auton, A., Abecasis, G., Albers, C.A., Banks, E., DePristo, M.A., Handsaker, R.E. *et al*. and 1000 Genomes Project Analysis Group. (2011) The variant call format and VCFtools. *Bioinformatics*, **27**, 2156–2158.

Dong, C., Wang, J., Yu, Y.U., Ju, L., Zhou, X., Ma, X., Mei, G. *et al*. (2019) Identifying functional genes influencing *Gossypium hirsutum* fiber quality. *Front Plant Sci.* **9**, 1968.

Du, X., Huang, G., He, S., Yang, Z., Sun, G., Ma, X., Li, N. *et al*. (2018) Resequencing of 243 diploid cotton accessions based on an updated A genome identifies the genetic basis of key agronomic traits. *Nat. Genet.* **50**, 796–802.

Fan, L., Wang, L., Wang, X., Zhang, H., Zhu, Y., Guo, J., Gao, W. *et al*. (2018) A high-density genetic map of extra-long staple cotton (*Gossypium barbadense*) constructed using genotyping-by-sequencing based single nucleotide polymorphic markers and identification of fiber traits-related QTL in a recombinant inbred line population. *BMC Genom.* **19**, 489.

Fang, L., Gong, H., Hu, Y., Liu, C., Zhou, B., Huang, T., Wang, Y. *et al*. (2017a) Genomic insights into divergence and dual domestication of cultivated allotetraploid cottons. *Genome Biol.* **18**, 33.

Fang, L., Wang, Q., Hu, Y., Jia, Y., Chen, J., Liu, B., Zhang, Z. *et al*. (2017b) Genomic analyses in cotton identify signatures of selection and loci associated with fiber quality and yield traits. *Nat. Genet.* **49**, 1089–1098.

Fang, L., Zhao, T., Hu, Y., Si, Z., Zhu, X., Han, Z., Liu, G. *et al*. (2021) Divergent improvement of two cultivated allotetraploid cotton species. *Plant Biotechnol. J.* **19**, 1325–1336.

Feng, H., Li, X., Chen, H., Deng, J., Zhang, C., Liu, J., Wang, T. *et al*. (2018) GhHUB2, a ubiquitin ligase, is involved in cotton fiber development via the ubiquitin-26S proteasome pathway. *J. Exp. Bot.* **69**, 5059–5075.

Gao, W., Long, L., Zhu, L.F., Xu, L., Gao, W.H., Sun, L.Q., Liu, L.L. *et al*. (2013) Proteomic and virus-induced gene silencing (VIGS) analyses reveal that gossypol, brassinosteroids, and jasmonic acid contribute to the resistance of cotton to *Verticillium dahliae*. *Mol Cell Proteomics*, **12**, 3690–3703.

Gong, W., Xu, F., Sun, J., Peng, Z., He, S., Pan, Z. and Du, X. (2017) iTRAQ-based comparative proteomic analysis of seedling leaves of two Upland cotton genotypes differing in salt tolerance. *Front Plant Sci.* **8**, 2113.

Gross, S.D. and Anderson, R.A. (1998) Casein kinase I: spatial organization and positioning of a multifunctional protein kinase family. *Cell Signal.* **10**, 699–711.

Grover, C.E., Arick, M.A., Thrash, A., Conover, J.L., Sanders, W.S., Peterson, D.G., Frelichowski, J.E. *et al*. (2019) Insights into the evolution of the new world diploid cottons (*Gossypium*, subgenus *houzingenia*) based on genome sequencing. *Genome Biol. Evol.* **11**, 53–71.

Grover, C.E., Pan, M., Yuan, D., Arick, M.A., Hu, G., Brase, L., Stelly, D.M. *et al*. (2020) The *Gossypium longicalyx* genome as a resource for cotton breeding and evolution. *Genes Genom. Genet.* **10**, 1457–1467.

Gu, Z., Huang, C., Li, F. and Zhou, X. (2014) A versatile system for functional analysis of genes and microRNAs in cotton. *Plant Biotechnol. J.* **12**, 638–649.

Ho, M.H., Saha, S., Jenkins, J.N. and Ma, D.P. (2010) Characterization and promoter analysis of a cotton RING-type ubiquitin ligase (E3) gene. *Mol. Biotechnol.* **46**, 140–148.

Hu, Y., Chen, J., Fang, L., Zhang, Z., Ma, W., Niu, Y., Ju, L. *et al*. (2019) *Gossypium barbadense* and *Gossypium hirsutum* genomes provide insights into the origin and evolution of allotetraploid cotton. *Nat. Genet.* **51**, 739–748.

Huang, C., Nie, X., Shen, C., You, C., Li, W., Zhao, W., Zhang, X. *et al*. (2017) Population structure and genetic basis of the agronomic traits of upland cotton in China revealed by a genome-wide association study using high-density SNPs. *Plant Biotechnol. J.* **15**, 1374–1386.

Huang, G., Wu, Z., Percy, R.G., Bai, M., Li, Y., Frelichowski, J.E., Hu, J. *et al*. (2020) Genome sequence of *Gossypium herbaceum* and genome updates of *Gossypium arboreum* and *Gossypium hirsutum* provide insights into cotton A-genome evolution. *Nat. Genet.* **52**, 516–524.

Huang, X. and Han, B. (2014) Natural variations and genome-wide association studies in crop plants. *Annu. Rev. Plant. Biol.* **65**, 531–551.

Huang, X., Kurata, N., Wei, X., Wang, Z.-X., Wang, A., Zhao, Q., Zhao, Y. *et al*. (2012) A map of rice genome variation reveals the origin of cultivated rice. *Nature*, **490**, 497–501.

Huang, X., Wei, X., Sang, T., Zhao, Q., Feng, Q.I., Zhao, Y., Li, C. *et al*. (2010) Genome-wide association studies of 14 agronomic traits in rice landraces. *Nat. Genet.* **42**, 961–967.

Islam, S., Thyssen, G.N., Jenkins, J.N., Zeng, L., Delhom, C.D., McCarty, J.C., Deng, D.D. *et al*. (2016) A MAGIC population-based genome-wide association study reveals functional association of *GhRBB1_A07* gene with superior fiber quality in cotton. *BMC Genom.* **17**, 903.

Jia, G., Huang, X., Zhi, H., Zhao, Y., Zhao, Q., Li, W., Chai, Y. *et al*. (2013) A haplotype map of genomic variations and genome-wide association studies of agronomic traits in foxtail millet (*Setaria italica*). *Nat. Genet.* **45**, 957–961.

Jiao, Y., Zhao, H., Ren, L., Song, W., Zeng, B., Guo, J., Wang, B. *et al*. (2012) Genome-wide genetic changes during modern breeding of maize. *Nat. Genet.* **44**, 812–815.

Kim, D., Langmead, B. and Salzberg, S. (2015) HISAT: a fast spliced aligner with low memory requirements. *Nat. Methods*, **12**, 357–360.

Kinoshita, A., Seo, M., Kamiya, Y. and Sawa, S. (2015b) Mystery in genetics: PUB4 gives a clue to the complex mechanism of CLV signaling pathway in the shoot apical meristem. *Plant Signal. Behav.* **10**, e1028707.

Kinoshita, A., ten Hove, C.A., Tabata, R., Yamada, M., Shimizu, N., Ishida, T., Yamaguchi, K. *et al*. (2015a) A plant U-box protein, PUB4, regulates asymmetric cell division and cell proliferation in the root meristem. *Development*, **142**, 444–453.

Li, C., Fu, Y., Sun, R., Wang, Y. and Wang, Q. (2018) Single-locus and multi-locus genome-wide association studies in the genetic dissection of fiber quality traits in Upland cotton (*Gossypium hirsutum* L.). *Front. Plant Sci.* **9**, 1083.

Li, F., Fan, G., Wang, K., Sun, F., Yuan, Y., Song, G., Li, Q. *et al*. (2014) Genome sequence of the cultivated cotton *Gossypium arboreum*. *Nat. Genet.* **46**, 567–572.

Li, F., Fan, G., Lu, C., Xiao, G., Zou, C., Kohel, R.J., Ma, Z. *et al*. (2015) Genome sequence of cultivated upland cotton (*Gossypium hirsutum* TM-1) provides insights into genome evolution. *Nat. Biotechnol.* **33**, 524.

Li, H. and Durbin, R. (2010) Fast and accurate long-read alignment with Burrows-Wheeler transform. *Bioinformatics*, **26**, 589–595.

Li, H., Handsaker, B., Wysoker, A., Fennell, T., Ruan, J., Homer, N., Marth, G. *et al*. and 1000 Genome Project Data Processing Subgroup. (2009) The sequence alignment/map format and SAMtools. *Bioinformatics*, **25**, 2078–2079.

Li, H., Peng, Z., Yang, X., Wang, W., Fu, J., Wang, J., Han, Y. *et al*. (2013) Genome-wide association study dissects the genetic architecture of oil biosynthesis in maize kernels. *Nat. Genet.* **45**, 43–50.

Li, P.T., Lu, Q.W., Xiao, X.H., Yang, R. and Duan, X.X. (2021) Dynamic expression analysis and introgressive gene identification of fiber length using chromosome segment substitution lines from *G. hirsutum* × *G. barbadense*. *J. Exp. Bot.* **90**, 129–144.

Li, Q., Hu, A., Qi, J., Dou, W., Qin, X., Zou, X., Xu, L. *et al*. (2020) CsWAKL08, a pathogen-induced wall-associated receptor-like kinase in sweet orange, confers resistance to citrus bacterial canker via ROS control and JA signaling. *Hortic. Res.* **7**, 42.

Liu, R., Gong, J., Xiao, X., Zhang, Z., Li, J., Liu, A., Lu, Q. *et al*. (2018) GWAS analysis and QTL identification of fiber quality traits and yield components in Upland cotton using enriched high-density SNP markers. *Front. Plant Sci.* **9**, 1067.

Liu, S., Zhang, X., Xiao, S., Ma, J., Shi, W., Qin, T., Xi, H. *et al*. (2021) A single-nucleotide mutation in a GLUTAMATE RECEPTOR-LIKE gene confers resistance to *Fusarium Wilt* in *Gossypium hirsutum*. *Adv. Sci.* **8**, 2002723.

Lu, Q., Shi, Y., Xiao, X., Li, P., Gong, J., Gong, W., Liu, A. *et al*. (2017) Transcriptome analysis suggests that chromosome introgression fragments from Sea Island cotton (*Gossypium barbadense*) increase fiber strength in upland cotton (*Gossypium hirsutum*). *Genes Genom. Genet.* **7**, 3469–3479.

Lu, X., Fu, X., Wang, D., Wang, J., Chen, X., Hao, M., Wang, J. *et al*. (2019) Resequencing of cv CRI-12 family reveals haplotype block inheritance and recombination of agronomically important genes in artificial selection. *Biotechnol. J.* **17**, 945–955.

Ma, J., Geng, Y., Pei, W., Wu, M., Li, X., Liu, G., Li, D. *et al*. (2018a) Genetic variation of dynamic fiber elongation and developmental quantitative trait locus mapping of fiber length in upland cotton (*Gossypium hirsutum* L.). *BMC Genom.* **19**, 882.

Ma, X., Wang, Z., Li, W., Zhang, Y., Zhou, X., Liu, Y., Ren, Z. *et al*. (2019) Resequencing core accessions of a pedigree identifies derivation of genomic segments and key agronomic trait loci during cotton improvement. *Plant Biotechnol. J.* **17**, 762–775.

Ma, Z., He, S., Wang, X., Sun, J., Zhang, Y., Zhang, G., Wu, L. *et al*. (2018b) Resequencing a core collection of upland cotton identifies genomic variation and loci influencing fiber quality and yield. *Nat. Genet.* **50**, 803–813.

Mace, E.S., Tai, S., Gilding, E.K., Li, Y., Prentis, P.J., Bian, L., Campbell, B.C. *et al*. (2013) Whole-genome sequencing reveals untapped genetic potential in Africa's indigenous cereal crop sorghum. *Nat. Commun.* **4**, 2320.

Malukani, K.K., Ranjan, A., Hota, S.J., Patel, H.K. and Sonti, R.V. (2020) Dual activities of receptor-like kinase OsWAKL21.2 induce immune responses. *Plant Physiol.* **183**, 1345–1363.

Mao, X., Cai, T., Olyarchuk, J.G. and Wei, L. (2005) Automated genome annotation and pathway identification using the KEGG Orthology (KO) as a controlled vocabulary. *Bioinformatics*, **21**, 3787–3793.

McKenna, A., Hanna, M., Banks, E., Sivachenko, A., Cibulskis, K., Kernytsky, A., Garimella, K. *et al*. (2010) The Genome Analysis Toolkit: a MapReduce framework for analyzing next-generation DNA sequencing data. *Genome Res.* **20**, 1297–1303.

Park, H.C., Kim, M.L., Lee, S.M., Bahk, J.D., Yun, D.J., Lim, C.O., Hong, J.C. *et al*. (2007) Pathogen-induced binding of the soybean zinc finger homeodomain proteins GmZF-HD1 and GmZF-HD2 to two repeats of ATTA homeodomain binding site in the calmodulin isoform 4 (GmCaM4) promoter. *Nucleic Acids Res.* **35**, 3612–3623.

Paterson, A.H., Wendel, J.F., Gundlach, H., Guo, H., Jenkins, J., Jin, D., Llewellyn, D. *et al*. (2012) Repeated polyploidization of *Gossypium* genomes and the evolution of spinnable cotton fibres. *Nature*, **492**, 423–427.

Percy, R.G. and Wendel, J.F. (1990) Allozyme evidence for the origin and diversification of *Gossypium barbadense* L. *Theor. Appl. Genet.* **79**, 529–542.

Poland, J.A., Bradbury, P.J., Buckler, E.S. and Nelson, R.J. (2011) Genome-wide nested association mapping of quantitative resistance to northern leaf blight in maize. *Proc. Natl Acad. Sci. USA*, **108**, 6893–6898.

Purcell, S., Neale, B., Todd-Brown, K., Thomas, L., Ferreira, M.A., Bender, D., Maller, J. *et al*. (2007) PLINK: a tool set for whole-genome association and population-based linkage analyses. *Am. J. Hum. Genet.* **81**, 559–575.

Shi, G., Guo, X., Guo, J., Liu, L. and Hua, J. (2015) Analyzing serial cDNA libraries revealed reactive oxygen species and gibberellins signaling pathways in the salt response of Upland cotton (*Gossypium hirsutum* L.). *Plant Cell Rep.* **34**, 1005–1023.

Splitstoser, J.C., Dillehay, T.D., Wouters, J. and Claro, A. (2016) Early pre-Hispanic use of indigo blue in Peru. *Sci. Adv.* **2**, e1501623.

Su, J., Li, L., Pang, C., Wei, H., Wang, C., Song, M., Wang, H. *et al*. (2016) Two genomic regions associated with fiber quality traits in Chinese upland cotton under apparent breeding selection. *Sci. Rep.* **6**, 38496.

Su, J., Ma, Q., Li, M., Hao, F. and Wang, C. (2018) Multi-locus genome-wide association studies of fiber-quality related traits in Chinese early-maturity Upland cotton. *Front. Plant Sci.* **9**, 1169.

Su, X., Zhu, G., Song, X., Xu, H., Li, W., Ning, X., Chen, Q. *et al*. (2020) Genome-wide association analysis reveals loci and candidate genes involved in fiber quality traits in Sea Island cotton (*Gossypium barbadense*). *BMC Plant Biol.* **20**, 289.

Sun, Z., Wang, X., Liu, Z., Gu, Q., Zhang, Y., Li, Z., Ke, H. *et al*. (2017) Genome-wide association study discovered genetic variation and candidate genes of fibre quality traits in *Gossypium hirsutum* L. *Plant Biotechnol. J.* **15**, 982–996.

Tyagi, P., Gore, M.A., Bowman, D.T., Campbell, B.T., Udall, J.A. and Kuraparthy, V. (2014) Genetic diversity and population structure in the US Upland cotton (*Gossypium hirsutum* L.). *Theor. Appl. Genet.*, **127**, 283–295.

Udall, J.A., Long, E., Hanson, C., Yuan, D., Ramaraj, T., Conover, J.L., Gong, L. *et al*. (2019) De novo genome sequence assemblies of *Gossypium raimondii* and *Gossypium turneri*. *Genes Genom. Genet.* **9**, 3079–3085.

Ulloa, M., Percy, R., Hutmacher, R.B. and Zhang, J. (2009) The future of cotton breeding in the Western United States. *J. Cotton Sci.* **13**, 246–255.

Wang, K., Li, M. and Hakonarson, H. (2010) ANNOVAR: functional annotation of genetic variants from high-throughput sequencing data. *Nucleic Acids Res.* **38**, e164.

Wang, K., Wang, Z., Li, F., Ye, W., Wang, J., Song, G., Yue, Z. *et al*. (2012) The draft genome of a diploid cotton *Gossypium raimondii*. *Nat. Genet.* **44**, 1098–1103.

Wang, K., Wendel, J. and Hua, J. (2018) Designations for individual genomes and chromosomes in *Gossypium*. *J. Cotton Res.* **1**, 3.

Wang, M., Tu, L., Lin, M., Lin, Z., Wang, P., Yang, Q., Ye, Z. *et al*. (2017a) Asymmetric subgenome selection and cis-regulatory divergence during cotton domestication. *Nat. Genet.* **49**, 579–587.

Wang, M., Tu, L., Yuan, D., Zhu, D., Shen, C., Li, J., Liu, F. *et al*. (2019) Reference genome sequences of two cultivated allotetraploid cottons, *Gossypium hirsutum* and *Gossypium barbadense*. *Nat. Genet.* **51**, 224–229.

Wang, Y., Wu, Y., Yu, B., Yin, Z. and Xia, Y. (2017b) EXTRA-LARGE G PROTEINs interact with E3 ligases PUB4 and PUB2 and function in cytokinin and developmental processes. *Plant Physiol.* **173**, 1235–1246.

Wendel, J.F., Brubaker, C.L. and Seelanan, T. (2010) The origin and evolution of *Gossypium*. In *Physiology of Cotton*, (Stewart, J.M., Oosterhuis, D.M., Heitholt, J.J. and Mauney, J.R., eds), pp. 1–18. Netherlands, Europe: Springer.

Wendel, J.F. and Grover, C.E. (2015) Taxonomy and evolution of the cotton genus, *Gossypium*. In *Cotton*, (Fang, D.D. and Percy, R.G., eds), pp. 25–44. New Jersey, US: John Wiley & Sons, Ltd.

Westengen, O.T., Huamán, Z. and Heun, M. (2005) Genetic diversity and geographic pattern in early South American cotton domestication. *Theor. Appl. Genet.* **110**, 392–402.

Xiao, G., Zhao, P. and Zhang, Y. (2019) A pivotal role of hormones in regulating cotton fiber development. *Front. Plant Sci.* **10**, 87.

Yang, Z., Ge, X., Yang, Z., Qin, W., Sun, G., Wang, Z., Li, Z. *et al.* (2019) Extensive intraspecific gene order and gene structural variations in upland cotton cultivars. *Nat. Commun.* **10**, 2989.

Yano, K., Yamamoto, E., Aya, K., Takeuchi, H., Lo, P.C., Hu, L., Yamasaki, M. *et al.* (2016) Genome-wide association study using whole-genome sequencing rapidly identifies new genes influencing agronomic traits in rice. *Nat. Genet.* **48**, 927–934.

Yao, Z., Chen, Q., Chen, D., Zhan, L., Zeng, K., Gu, A., Zhou, J. *et al.* (2019) The susceptibility of sea-island cotton recombinant inbred lines to *Fusarium oxysporum* f. sp. *vasinfectum* infection is characterized by altered expression of long noncoding RNAs. *Sci. Rep.* **9**, 2894.

Young, M.D., Wakefield, M.J., Smyth, G.K. and Oshlack, A. (2010) Gene ontology analysis for RNA-seq: accounting for selection bias. *Genome Biol.* **11**, R1.

Yu, J., Hui, Y., Chen, J., Yu, H., Gao, X., Zhang, Z., Li, Q. *et al.* (2021) Whole-genome resequencing of 240 *Gossypium barbadense* accessions reveals genetic variation and genes associated with fiber strength and lint percentage. *Theor. Appl. Genet.* **134**, 3249–3261.

Yu, J., Zhang, K., Li, S., Yu, S., Zhai, H., Wu, M., Li, X. *et al.* (2013) Mapping quantitative trait loci for lint yield and fiber quality across environments in a *Gossypium hirsutum* × *Gossypium barbadense* backcross inbred line population. *Theor. Appl. Genet.* **126**, 275–287.

Yuan, D., Grover, C.E., Hu, G., Pan, M., Miller, E.R., Conover, J.L., Hunt, S.P. *et al.* (2021) Parallel and intertwining threads of domestication in allopolyploid cotton. *Adv. Sci.* **8**, 2003634.

Yuan, D., Tang, Z., Wang, M., Gao, W., Tu, L., Jin, X., Chen, L. *et al.* (2015) The genome sequence of Sea-Island cotton (*Gossypium barbadense*) provides insights into the allopolyploidization and development of superior spinnable fibres. *Sci. Rep.* **5**, 17662.

Zhang, J., Fang, H., Zhou, H., Sanogo, S. and Ma, Z. (2014) Genetics, breeding, and marker-assisted selection for *Verticillium Wilt* resistance in cotton. *Crop Sci.* **54**, 1289–1303.

Zhang, T., Hu, Y., Jiang, W., Fang, L., Guan, X., Chen, J., Zhang, J. *et al.* (2015) Sequencing of allotetraploid cotton (*Gossypium hirsutum* L. acc. TM-1) provides a resource for fiber improvement. *Nat. Biotechnol.* **33**, 531–537.

Zhang, X., Hu, D., Li, Y., Chen, Y., Abidallha, E.H.M.A., Dong, Z., Chen, D. *et al.* (2017) Developmental and hormonal regulation of fiber quality in two natural-colored cotton cultivars. *J. Integr. Agric.* **16**, 1720–1729.

Zhao, Y., Wang, H., Chen, W. and Li, Y. (2014) Genetic structure, linkage disequilibrium and association mapping of *Verticillium wilt* resistance in elite cotton (*Gossypium hirsutum* L.) germplasm population. *PLoS One*, **9**, e86308.

Zhou, X. and Stephens, M. (2012) Genome-wide efficient mixed-model analysis for association studies. *Nat. Genet.* **44**, 821–824.

Zhou, Z., Jiang, Y.U., Wang, Z., Gou, Z., Lyu, J., Li, W., Yu, Y. *et al.* (2015) Resequencing 302 wild and cultivated accessions identifies genes related to domestication and improvement in soybean. *Nat. Biotechnol.* **33**, 408–414.

Supporting information

Additional supporting information may be found online in the Supporting Information section at the end of the article.

Figure S1 Geographic distribution of 336 Sea Island cotton accessions.

Figure S2 Genetic diversity, mean Ln*P*(D), Δ*K* value, PCA analysis, phylogenetic tree and structure analyses.

Figure S3 Frequency distribution and correlation coefficients of phenotypic variations of 15 traits.

Figure S4 Genome-wide association study of fibre length (FL).

Figure S5 Genome-wide association study of fibre uniformity (FU).

Figure S6 Genome-wide association study of fibre strength (FS).

Figure S7 Genome-wide association study of fibre elongation (FE).

Figure S8 Genome-wide association study of fibre micronaire (FM).

Figure S9 Genome-wide association study of fruit branch number (FBN).

Figure S10 Genome-wide association study of boll number (BN).

Figure S11 Genome-wide association study of single boll weight (SBW).

Figure S12 Genome-wide association study of lint percentage (LP).

Figure S13 Genome-wide association study of seed index (SI).

Figure S14 Genome-wide association study of disease percentage (DP).

Figure S15 Genome-wide association study of growth period (GP).

Figure S16 Genome-wide association study of the first node of fruit branch (FNFB).

Figure S17 Genome-wide association study of plant height (PH).

Figure S18 Genome-wide association study of fruit branch type (FBT).

Figure S19 Identification of the FS causal gene *GbFS1* on chromosome Dt11.

Figure S20 Number of China Sea Island accessions with different haplotype combinations.

Figure S21 Identification of the DP causal gene *GbDP1* on chromosome Dt03.

Figure S22 Overlapped genes between GWAS and genetic transmission analysis.

Figure S23 Flowchart showing the hierarchical filtering strategy of associated SNPs/genes, QTL, candidate/key genes.

Table S1 336 Sea Island cotton accessions and their sequenced information in our study.

Table S2 Information of tetraploid cotton genomes in recent GWAS studies and their referenced genomes.

Table S3 Statistics of different SNP mutation types for 336 accessions.

Table S4 Summary of categorized InDels.

Table S5 Summary of the number of SNPs and nucleotide diversity.

Table S6 The ancestry proportion estimates for each accession.

Table S7 Tracy-Widom statistics of eigenvalues from PCA analysis.

Table S8 The ecological characteristics of four locations for phenotyping.

Table S9 Phenotypic data of the 15 traits.

Table S10 List of the associated SNPs and genes for 15 traits.

Table S11 Statistics of the associated SNP number for 15 traits.

Table S12 Statistics of the associated gene number for 15 traits.

Table S13 China accessions with different haplotype combination.

Table S14 Selective pressure analysis based on *Ka* and *Ks* value.
Table S15 Genetic constitutions of XH39 and XH60.
Table S16 The same genes related to key traits in XH39 and XH60 pedigree identified by both GWAS and IBD analysis.
Table S17 Comparison of genome sequencing data in common Sea Island cotton samples in our and other studies.
Table S18 Comparison of fibre quality and yield phenotype data in our and other studies.
Table S19 Loci and genes for fibre length and fibre strength which overlap with previous researches on *G. barbadense*.
Table S20 Primers used in this study.
Table S21 Fibre samples of Sea Island cotton used for transcriptome sequencing and analysis.